

PERFORMANCE ANALYSIS OF MULTIUSER FREE SPACE OPTICAL COMMUNICATIONS

A Thesis

by

Sasan Zhalehpour

Submitted to the
Graduate School of Sciences and Engineering
In Partial Fulfillment of the Requirements for
the Degree of

Master of Science

in the
Department of Electrical and Electronics Engineering

Özyeğin University
August 2014

Copyright © 2014 by Sasan Zhalehpour

PERFORMANCE ANALYSIS OF MULTIUSER FREE SPACE OPTICAL COMMUNICATIONS

Approved by:

Professor Murat Uysal, Advisor
Department of Electrical and Electronics
Engineering
Özyeğin University

Professor Cenk Demirođlu
Department of Electrical and Electronics
Engineering
Özyeğin University

Professor Sultan Aldirmaz
Department of Electrical and Electronics
Engineering
Kocaeli University

Date Approved: 13 August 2014

*To my dear parents,
Afsar and Akbar Zhalehpour
and
my beloved sister,
Sara*

ABSTRACT

Terrestrial Free Space Optical (FSO) communications involve using optical beams to carry information through atmospheric channels between two points. Unlike radio frequency (RF) communications, FSO systems are not burdened by spectrum licensing or interference to/from other systems. These systems are also easy-to-install and redeployable, therefore considered a powerful alternative to fiber optic or RF systems, particularly, for the purpose of last mile problem. In addition, the nature of point to point transmission by means of laser beam provides high immunity to interference and jamming from external sources.

In the first chapter of the thesis, we provide an overview of FSO technology discussing the advantages and bottlenecks as well as mitigation techniques in FSO systems to overcome atmospheric turbulence induced fading problem.

In the second chapter, we consider a multiuser FSO system over log-normal atmospheric turbulence channels. We investigate the outage probability of proposed system with various scheduling techniques including Round Robin, Opportunistic Round Robin, Select-Max and m^{th} Best User Selection. We also verify the validity of the obtained closed-form expressions for outage probabilities through Monte Carlo simulations.

In the third chapter, we extend the multiuser scenario to a parallel multihop (cooperative) FSO system and study its outage probability with the so-called m^{th} Best Path Selection (m-BPS) protocol. Specifically, we consider an FSO communication system which employs M parallel relaying paths each of which consists of N decode-and-forward relays. In this protocol, data is transmitted through the m^{th} ($m \geq 2$) best path towards the destination since the best path (i.e., $m = 1$) might not be

available due to scheduling or load balancing issues. After expressing closed-form of outage capacity, we derive the diversity order of proposed system.

In the last chapter, we derive outage capacity and throughput expressions for the multiuser FSO system under consideration. These expressions are obtained under the assumption of both independent identical and non-identical distributions assuming log-normal channel model and then confirmed through simulation results.

Özetçe

Kablosuz optik (free space optical, FSO) haberleşme sistemleri iki nokta arasındaki atmosferik kanal aracılığı ile optik hüzmeleri kullanarak iletim sağlar. Radyo frekansı (RF) iletiminden farklı olarak, FSO sistemler spektrum lisansı gerektirmezler ve diğer sistemlerden kaynaklı girişim gibi problemler barındırmazlar. Bu sistemler kolay kurulabilir ve tekrar kullanılabilir özellikte olduklarından fiber optik ve RF sistemlerine – özellikle “son mil” problemi için – alternatif bir çözüm olarak karşımıza çıkmaktadırlar. Ek olarak, lazer hüzmeleri ile uçtan uca iletimin doğası girişim ve dış kaynaklı boğmalara karşı bağımsızlık göstermektedir.

Tezin ilk bölümünde FSO teknolojisinin avantajları ve sıkıntıları hakkında genel bir inceleme sunacağız. Bunun yanında, FSO sistemlerinde atmosferik türbülansdan kaynaklanan sönümlenme probleminin nasıl aşılabileceğinden bahsedeceğiz.

İkinci bölümde, log-normal atmosferik türbülans kanalı üzerinde çalışan çok kullanıcılı bir FSO sistemini ele alacağız. Önerilen sistemi, farklı çizgeleme teknikleri (Round Robin, Fırsatçı Round Robin, En İyi Seçim ve m 'inci En İyi Seçim) altındaki hizmet kesinti olasılıklarını inceleyeceğiz. Elde edilen kapalı formdaki hizmet kesinti olasılıklarını Monte Carlo simülasyonları ile de doğrulayacağız.

Üçüncü bölümde, ikinci bölümdeki senaryoyu paralel çok-atlamalı (işbirlikli) FSO sistemine genişletireceğiz ve hizmet kesinti olasılığının çıkarımını m 'inci En İyi Yol Seçimi (m-BPS) protokolü altında yapacağız. Çalışmada her bir yolu N çözümlerle-ve-ilet rölesi içeren M paralel aktarma yolundan oluşan bir FSO sistemi varsaymaktayız. Bu protokolle, mevcut en iyi yol ($m=1$) çizgeleme ve yük dengeleme gereği iletme imkan veremediğinde, veri m 'inci ($m \geq 2$) yoldan hedefe iletilmektedir. Hizmet kesinti kapasitesinin kapalı formunu elde ettikten sonra, önerilen sistemin çeşitleme kazancını da bulmaktayız.

Son bölümde, çok kullanıcılı FSO sistemlerde hizmet kesinti kapasitesini ve iş çıkarma oranı ifadelerini elde edeceğiz. Bu çıkarımlar hem bağımsız özdeş, hem de özdeş olmayan log-normal kanal modelleri varsayımı ile elde edilmekte ve simülasyonlar ile doğrulanmaktadır.

ACKNOWLEDGEMENTS

Though only my name appears on the cover of this dissertation, a great many people have contributed to its production. First and foremost, I would like to express my deepest and profound gratitude to my supervisor professor Murat Uysal for his excellent guidance, patience, motivation, enthusiasm, and immense knowledge through my master program. I have been amazingly fortunate to have him as an advisor who gave me the freedom to explore on my own, and at the same time the guidance to recover when my steps faltered. Professor Murat Uysal taught me how to question thoughts and express ideas.

I would also like to thank my parents, and my sister, Sara. They were always supporting me and encouraging me with their best wishes.

Finally, my sincere thanks also goes my friends, Hosein Kazemi, Mahsa Fourah-nadeh, Elham Sarbazi and Zohreh Mostaani, who as good friends, were always willing to help and give me their best suggestions.

This project is financially supported by Tubitak Research Grant 111E143.

TABLE OF CONTENTS

DEDICATION	iii
ABSTRACT	iv
ÖZETÇE	vi
ACKNOWLEDGEMENTS	viii
LIST OF TABLES	xi
LIST OF FIGURES	xii
I OPTICAL WIRELESS COMMUNICATIONS	1
1.1 Introduction	1
1.2 Advantages and Applications of FSO	1
1.3 Atmospheric Turbulence channel Model	2
1.4 Fading Mitigation Techniques	4
1.4.1 Receive Diversity	4
1.4.2 Transmit Diversity	5
1.4.3 MIMO FSO Systems	5
1.4.4 Relay-assisted FSO systems	6
1.4.5 Multiuser diversity	7
1.5 Thesis structure and contributions	8
II OUTAGE PROBABILITY ANALYSIS OF MULTIUSER FSO SYSTEMS	10
2.1 Introduction	10
2.2 System Model	10
2.3 Calculation of received SNR	12
2.4 Scheduling techniques	13
2.4.1 Round Robin Scheduling	13
2.4.2 Opportunistic Round Robin method	14
2.4.3 Select-max	14

2.4.4	m^{th} Best Selection	15
2.5	Outage Probability Analysis	16
2.5.1	Outage Probability Analysis of RR	16
2.5.2	Outage Probability Analysis of ORR	17
2.5.3	Outage Probability Analysis of select-max	17
2.5.4	Outage Probability Analysis of m^{th} Best Selection	17
2.5.5	Numerical Results and Discussions	18
III OUTAGE PROBABILITY ANALYSIS OF MULTIHOP PARALLEL FSO SYSTEMS		22
3.1	Introduction	22
3.2	System Model	22
3.3	Outage Probability Analysis	25
3.4	Diversity Order Analysis	26
3.5	Numerical Results and Discussions	28
IV OUTAGE CAPACITY ANALYSIS OF MULTIUSER FSO SYSTEM		32
4.1	Introduction	32
4.2	System Model	33
4.3	Outage Capacity Analysis	34
4.3.1	Independent Non Identical Distribution	36
4.3.2	Independent Identical Distribution	37
4.4	Numerical Results and Discussions	39
V CONCLUSION		43
REFERENCES		45
VITA		52

LIST OF TABLES

1	FSO system configuration	29
---	------------------------------------	----

LIST OF FIGURES

1	MU-MIMO FSO system including one transmitter and N users, each of which equipped with M_t and M_r transmit and receive apertures, respectively.	11
2	Outage performance of MU-MIMO FSO system with 1 st (select-max), 2 nd best user selection, ORR and RR scheduling policies. Assuming $N = 8$ and $M_t = 2$ and $M_r = 2$. As a benchmark, the performance of multiuser SISO scenario ($N = 8$ and $M_t = 1$ and $M_r = 1$) is included.	20
3	Outage performance of MU-MIMO FSO system with 1 st (select-max), 2 nd , ORR and RR scheduling policies with respect to the number of users is presented, assuming $N = 8$ and $M_t = 2$ and $M_r = 2$	21
4	FSO system with M paths each of which consists of N relay nodes.	23
5	Outage performance of FSO system with 1 st , 2 nd , 3 rd and 4 th best path selection assuming $M = 4$ and $N = 3$. As a benchmark, the performance of serial relaying path ($M = 1$ and $N = 3, 2, 1$) along with direct path communication ($M = 1$ and $N = 0$) are included.	28
6	Outage performance of iid and inid FSO system with 1 st , 2 nd , 3 rd and 4 th best path selection assuming $M = 4$ and $N = 3$	30
7	RDO and ARDO comparison of FSO system by m-BPS.	31
8	FMultiuser SISO FSO system with one transmitter and N users.	34
9	Outage Capacities of Multiuser FSO system, considering max-select scheduling protocol with $N = 10$ have been shown for iid cases of $d = 2.5$ km and $d = 3.5$ km. Furthermore the inid case of placing users over the boundary of 2.5 km to 3.5 km along with the lower bound of corresponding outage capacities are presented.	40
10	Outage Capacities of Multiuser FSO system, assuming max-select scheduling protocol with $N = 10$ are included for iid cases of $d = 2.5$ km and $d = 3.5$ km along with the lower bound of each outage capacity.	41
11	Outage Capacities of multiuser FSO system, assuming max-select scheduling protocol with respect to the number of users are shown for iid cases of $d = 2.5$ km and $d = 3.5$ km within low and high SNR regimes (-5 dB and 15 dB).	42

CHAPTER I

OPTICAL WIRELESS COMMUNICATIONS

1.1 Introduction

Free-space optical communication (FSO) uses laser transmitters to enable wireless connectivity between two distant points. In this chapter, we provide a brief overview of FSO systems including its distinctive features and application areas. Then, we discuss the main drawbacks of FSO systems and potential solutions to overcome those issues.

1.2 Advantages and Applications of FSO

FSO systems are used for high data rate communication between two fixed points over distances up to several kilometers. In comparison to radio frequency (RF) counterparts, the FSO link has a very high optical bandwidth available, allowing much higher data rates. Terrestrial FSO products with transmission rates of 10Gb/sec are already in the market [1] and the speeds of recent experimental WOC systems are competing with fiber optic [2–6]. FSO systems use very narrow laser beams. This spatial confinement provides a high reuse factor, an inherent security, and robustness to electromagnetic interference. Furthermore, the frequency in use by the FSO technology is above 300 GHz which is unlicensed worldwide. Therefore, FSO systems do not require license fees [7]. FSO systems are also easily deployable and can be reinstalled without the cost of dedicated fiber optic connections.

FSO systems have initially attracted attention as an efficient solution for the last mile problem to bridge the gap between the end user and the fiber optic infrastructure already in place. Telecom carriers have already made substantial investments

to augment the capacity of their fiber backbones. To fully utilize the existing capacity, and therefore generate revenue, this expansion in the backbone of the networks should be accompanied by a comparable growth at the network edge where end users get access to the system. FSO systems can be also used for a number of long-range communication applications including cellular backhauls, wireless metropolitan area network (WMAN) extensions, WLAN-to-WLAN connectivity in enterprise and campus environments, broadband access to remote or underserved areas, and wireless video surveillance/monitoring. Since FSO links are easy-to-install and redeployable, they are particularly useful as redundant links in disaster situations where local infrastructure could be damaged or unreliable.

1.3 Atmospheric Turbulence channel Model

Atmospheric turbulence is caused by variation in the refractive index along the transmission link, which consequently leads into random fluctuations in the intensity and the phase of the received signal. These intensity fluctuations, called fading or scintillation, can result in a considerable degradation of the FSO system performance [8,9].

Atmospheric turbulence can be classified into different categories including weak, moderate and strong regimes [10]. Several statistical models have been introduced to describe the atmospheric turbulence within these regimes. The most commonly accepted models are log-normal and Gamma-Gamma turbulence models. The former one is mainly limited to weak turbulence conditions while the latter is applicable to a wider range of turbulence conditions [9].

Scintillation index is commonly used to describe the turbulence strength. It is defined as the normalized variance of irradiance fluctuations [9] and given by

$$\sigma_I^2 = \frac{E[I^2] - (E[I])^2}{(E[I])^2} = \frac{E[I^2]}{(E[I])^2} - 1 \quad (1)$$

where I represents the instantaneous optical irradiance (i.e., power density of the optical beam) and $E[\cdot]$ is the expectation function

Under the consideration of clear-sky, atmospheric turbulence with several hundred meters propagation distance can be modeled via a log-normal distribution channel [11, 12]. The range of scintillation index for lognormal channel model is assumed to be less than unity, i.e., $\sigma_I^2 < 1$ [9].

For weak turbulence, log-normal probability distribution function (PDF) of the irradiance (power density of the received optical beam on the photodetector) can be expressed as

$$f(I) = \frac{1}{I\sqrt{2\pi\sigma_I^2}} \exp\left(-\frac{(\ln(I) - \mu)^2}{2\sigma_I^2}\right), I > 0 \quad (2)$$

where we assume $\mu = -0.5\sigma_I^2$ to ensure that the fading does not attenuate or amplify the average power.

In weak turbulence regimes, the scintillation index is proportional to the Rytov variance, which is defined as $\sigma_R^2(d) = 1.23C_n^2 k^{7/6} d^{11/6}$. Based on the wave type, this relation can be described for a spherical wave, i.e., $\sigma_{I,\text{sp}}^2(d)$ and plane wave, i.e., $\sigma_{I,\text{pl}}^2(d)$ as [13]

$$\sigma_{I,\text{pl}}^2(d) = \sigma_R^2 = 1.23C_n^2 k^{7/6} d^{11/6} \quad (3)$$

$$\sigma_{I,\text{sp}}^2(d) = 0.4\sigma_R^2 = 0.5C_n^2 k^{7/6} d^{11/6} \quad (4)$$

Here, C_n^2 denotes the index of refraction structure parameter in $\text{m}^{-2/3}$, $k = 2\pi/\lambda_w$ is the optical wave number where λ_w presents the wavelength, and d is distance length between the transmitter and the receiver [1]. C_n^2 is an altitude-dependent variable [14] and given by

$$C_n^2 = 0.00594 \left(\frac{v}{27}\right)^2 (h \times 10^{-5})^{10} e^{\frac{h}{1000}} + 2.7e^{\frac{-h}{1500}} \times 10^{-6} + A_c e^{\frac{-h}{1000}} \quad (5)$$

where v is the root-mean-square wind speed in meters per second, h is the altitude in meters, and A_c is a nominal value of C_n^2 at the ground. Typically, the value of C_n^2 varies from approximately $10^{-17}\text{m}^{-2/3}$ for weak turbulence conditions to $10^{-13}\text{m}^{-2/3}$ for strong turbulence conditions [15].

1.4 Fading Mitigation Techniques

Several approaches have been proposed to mitigate the fading effects of atmospheric turbulence. These include error control coding in conjunction with interleaving [16–18], maximum likelihood sequence detection (MLSD) with the knowledge of joint temporal statistics of the turbulence [19], diversity techniques [20], multiuser schemes [21, 22] and relay-assisted communications [23–27].

Due to high temporal correlation in FSO communications, channel coding requires large-size interleavers to achieve the promised coding gains. MLSD also comes with some practical limitations such as complicated multidimensional integrations along with high computational complexity [28].

Spatial diversity can be deployed through implementing multiple apertures at the receiver side known as Single Input Multiple Output (SIMO) [13, 21, 29, 30], multiple transmit apertures at the transmitter side known as Multiple Input Single Output (MISO) [31, 32], or a combination of the two former schemes known as Multiple Input Multiple Output (MIMO) technique [33–36]. In what follows, we briefly review the mentioned spatial techniques.

1.4.1 Receive Diversity

Unlike the RF systems, FSO transmission can offer diversity gains at the receiver side without using multiple receive compartments. One feasible way to provide such a gain is to use a relatively large lens to average over received intensity fluctuations. This method is mostly known as aperture averaging which is inherently obtained from receive diversity. This technique can be efficiently employed if the receiver lens aperture is larger than the fading correlation length [37]. Aperture averaging has already been studied in both theoretical and practical applications. In [7, 13], it is indicated that substantial scintillation reduction can be achieved even in the scenarios of moderate-to-strong turbulence conditions.

In case of SIMO FSO systems where we have multiple apertures at the receive side, wide variety of diversity techniques can be implemented for instance, equal gain combining (EGC) and optimal maximal-ratio combining (MRC). The former method takes the advantage of lower implementation complexity while the latter one needs channel state information (CSI) at the receive side. Moreover, the obtained performance of both EGC and MRC is so close to each other [21, 28].

1.4.2 Transmit Diversity

In case of MISO FSO scenarios, we simply duplicate the transmit signal over multiple optical beams which is known as repetition coding (RC). This method improves the reliability of the transmission at the receive side and also can be considered as promising method to reduce fading effects. Furthermore, it is shown in [38, 39] that in the presence of CSI at the transmitter, we can exploit the selection transmit diversity to achieve full diversity of the system. On the contrary, in case of imperfect CSI at the transmitter, different transmission techniques are applicable to still keep the performance of system acceptable [40]. On the other hand, through using more complex signaling schemes, we can enhance the coding gain in addition to the diversity order. For instance, in [41], transmit laser selection and space time trellis coding is introduced.

In MISO FSO system which also known as SIMO system employing EGC at the receiver within independent fading, the received intensity can be easily modeled by a different channel distributions divided by the number of sub-channels [13, 31, 42].

1.4.3 MIMO FSO Systems

MIMO technique is an effective method to exploit the fading over multipath channels which can provide multiplexing gain or improve diversity order of the system [43]. In FSO context, MIMO systems are usually applied to mitigate the turbulence-induced fading effect through transmitting signal over multiple fading paths (equivalently,

RC method). Some examples of implementing MIMO techniques are provided in [34, 36, 44, 45].

1.4.4 Relay-assisted FSO systems

Relay-assisted FSO systems have been introduced in the literature as an effective method to extend coverage and mitigate the effects of fading [46, 47]. In parallel FSO relaying [48], due to the line-of-sight requirement, the source is equipped with a multi-laser transmitter with each of the transmitter pointing out in the direction of a corresponding relay node. To avoid strict synchronization requirements, which might be particularly problematic for high data rates under consideration, relay selection has been further studied in [25, 26]. In [25], a parallel dual-hop FSO system was considered with Poisson noise over lognormal and Rayleigh fading channel models. The authors investigated select-max protocol which refers to the selection of the relay with the highest instantaneous signal-to-noise ratio (SNR). In [26], authors assumed a parallel dual-hop FSO system with Gaussian noise and investigated the performance of three relay selection protocols, namely select-max, all-active and distributed switch-and-stay over Gamma-Gamma turbulence channels.

In practice, the best relay, i.e., the one with the highest instantaneous SNR, might not be available for transmission due to some problems such as scheduling error, defective relay or load balancing. Scheduling error is a result of erroneous relay selection caused by imperfect channel estimation. In a practical system, channel estimation needs to be carried out to determine the link quality and identify the relay which gives the highest instantaneous SNR. As a result of imperfect channel estimation, the instantaneous SNR can be estimated with error and it might be possible to select another relay instead of the actual best one. Another possible problem is defective relay. If the best relay, for some reasons, breaks down or malfunctions, we might need to resort to another relay. On the other hand, load balancing can be a concern in a

multiuser system where multiple destinations are served through the same relay. To address such issues, the so-called m th best relay selection was proposed in the context of radio-frequency (RF) communication [49].

1.4.5 Multiuser diversity

In addition, to the above mentioned techniques, in a point-to-multipoint wireless system, multiuser diversity can also be exploited to provide multiuser diversity gain which can improve the system throughput and hence the link reliability. The basic idea behind implementing multiuser diversity is to take advantage of the channel fluctuations to obtain a certain performance gain, particularly when implementing MIMO technique can be challenging due to the restriction on using multiple antennas at the transmitter/receiver [50]. The multiuser diversity gain relies on disparate channels between users, so higher diversity gain can be achieved by having larger dynamic range of fading. Furthermore, the performance can be improved with the number of independent channels. Therefore, multiuser diversity is most effective in systems with a large number of users [51].

In multiuser diversity method, at any time slot, there are some users which have higher channel gain compared to the rest and by allocating system resources, i.e., power, to those users, we would be able to improve the system performance. In RF context, multiuser diversity has been firstly introduced in [52, 53] as a technique to increase sum of rates capacity and decrease probability of error in uplink and downlink channels with full CSI.

Since the performance of FSO systems strongly depends on the atmospheric conditions and path loss effects, multiuser diversity can be potentially used in FSO systems as well. In the recent papers, multiuser diversity techniques have been employed in the context of FSO communications based on Time Division Multiple Access (TDMA) fashion in which the transmission channel is allocated to the user in each time slot

based on their channel quality. In [54], the performance of the FSO system over log-normal channel model for various multiuser diversity scheduling schemes from the throughput and the latency perspectives has been studied. It has been shown that although select-max technique could outperform the rest of the scheduling policies regarding throughput, Proportional Fair Scheduling with Exponential Rule (PFS/ER) scheme achieves the minimum latency and higher fairness among users at the cost of lower throughput. In [50], another scheduling technique called N^{th} best selection has been addressed in which channel fluctuations can be effectively exploited to increase a selection diversity gain over both log-normal and gamma-gamma channel model.

Multiuser diversity explores several advantages including simpler receiver structure, i.e., single antenna per receiver is sufficient. In contrast, multiuser diversity techniques suffers from some drawbacks for instance, unfairness among users although it is possible to provide long-term fairness through channel normalization and/or employ historical throughput information. Also, requiring CSI state at the transmitter side for selection purpose in another challenging issue for multiuser system [55].

1.5 Thesis structure and contributions

This thesis is organized as follows: in Chapter 2, we consider several scheduling policies including Round Robin, Opportunistic Round Robin, Select-max and m^{th} best user selection in a multiuser MIMO FSO system. Under the assumption of log-normal turbulence, we derived the closed-form of outage probability expressions of the proposed systems. The derived expressions are further confirmed through Monte Carlo simulation results.

In chapter 3, we extend our work to parallel multihop relaying systems (cooperative communications). Specifically, we consider an FSO communication system which employs M parallel relaying paths each of which consists of N decode-and-forward relays. We exploit the so-called m^{th} best path selection (m-BPS) protocol for the

purpose of data transition through the m^{th} ($m \geq 2$) best path towards the destination since the best path (i.e., $m=1$) might not be available due to scheduling or load balancing issues. Under the assumption of log-normal turbulence channels, we derive a closed-form outage probability expression for the FSO communication system with m-BPS protocol and demonstrate that a diversity gain of $(M-m+1)(N+1)^{11/6}$ is available. The derived expressions are further validated by Monte Carlo simulation technique.

As data rates increase, slow fading channels become more appropriate model to describe optical communications channels. Regarding the information theory aspect, this is equivalent to communication over channels where there is a nonzero probability that any given transmission rate cannot be supported by the channel. Unlike the fast fading channel model, due to the delay constraints and coherence time within slow fading channels which prevent averaging over deep and shallow channel gains, it is possible that the fading becomes so severe that the instantaneous capacity is below any desired rate. As a result, a more realistic measure of a capacity is the probability that the channel can support a target rate. Thus, in chapter 4, we focus on outage capacity as another metric to measure the performance of the proposed multiuser FSO systems.

CHAPTER II

OUTAGE PROBABILITY ANALYSIS OF MULTIUSER FSO SYSTEMS

2.1 Introduction

In this chapter, we consider a Multiuser MIMO FSO system (MU-MIMO FSO) and study the performance of several scheduling techniques over log-normal turbulence channels. Specifically, we consider Round Robin, Opportunistic Round Robin, Select-max and m^{th} best user selection techniques and obtain the closed-form outage probability expressions for each of them. The accuracy of derived expressions are further confirmed through Monte Carlo simulations

2.2 System Model

As illustrated in Fig. 1, we consider a MU-MIMO FSO system with one transmit node and N active users where the transmitter and each user are respectively equipped with M_t and M_r apertures. At any given time slot, based on the available channel state information, the transmitter schedules one of the users according to the deployed scheduling policy.

We assume binary pulse position modulation (BPPM). Let $r_{s_{i,j}}^k$ and $r_{n_{i,j}}^k$, $i = 1, \dots, M_t$ and $j = 1, \dots, M_r$, respectively, denote the received electrical signals over the signal and non-signal slots of BPPM pulse from the i^{th} transmit aperture to the j^{th} receive aperture of the k^{th} user [47]. They are expressed as

$$r_{s_{i,j}}^k = RT_b (P_t g_{i,j}^k + P_b) + n_{s_{i,j}}^k \quad (6)$$

$$r_{n_{i,j}}^k = RT_b P_b + n_{n_{i,j}}^k \quad (7)$$

where R represents the responsivity of the photodetector and T_b is the duration of signal/non-signal slots in (8) and (9). P_t indicates the average transmitted optical power. P_b represents the background power on the photodetector. $n_{s_{i,j}}^k$ and $n_{n_{i,j}}^k$ denote the AWGN terms for the signal and non-signal slots which are modeled with zero mean and variance of $\sigma_n^2 = N_o/2$. The channel gain $g_{i,j}^k$ is defined as [47]

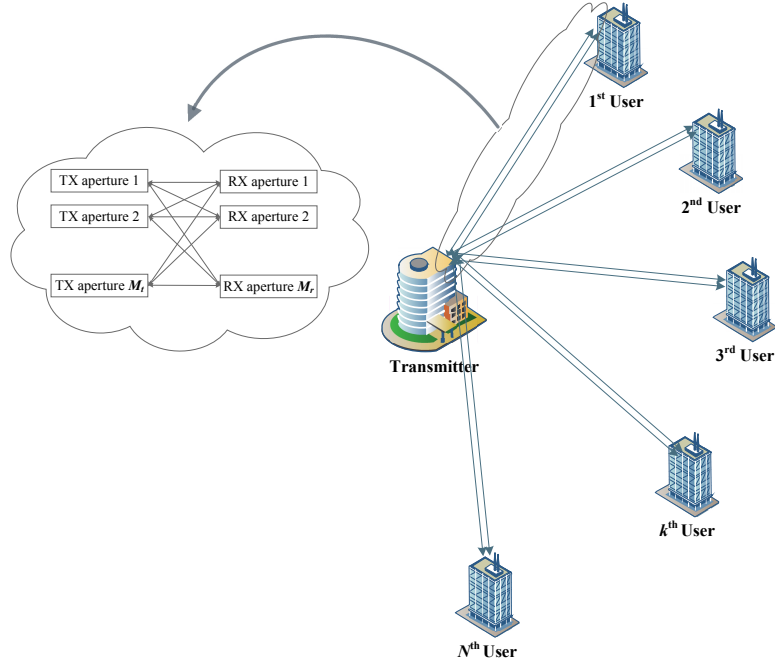


Figure 1: MU-MIMO FSO system including one transmitter and N users, each of which equipped with M_t and M_r transmit and receive apertures, respectively.

$$g_{i,j}^k = L(d_{i,j}^k) |\alpha_{i,j}^k|^2, \quad k=1, \dots, N, \quad i=1, \dots, M_t \quad \text{and} \quad j=1, \dots, M_r \quad (8)$$

where $L(d_{i,j}^k) = l(d_{i,j}^k)/l(d_{\max})$ denotes the normalized path loss with respect to the distance of the longest link between the transmitter and k^{th} user. The path loss $l(d_{i,j}^k)$ is given by $l(d_{i,j}^k) = e^{-\tau d_{i,j}^k} A_{TX} A_{RX} / (\lambda d_{i,j}^k)^2$ where A_{TX} and A_{RX} are transmit and receive aperture area, respectively and τ is the attenuation coefficient determined by the exponential Beers-Lambert law [56]. We assume that all links between the transmit and the receive apertures of each transmitter-user pair are

equidistant. Hence, we can conclude that $(d^k) = e^{\tau(d_{\max}-d^k)}(d_{\max}/d^k)^2$ is applicable for all users. For the system under consideration, we further assume that all users are placed equidistantly from the transmitter (iid distribution). Thus, the corresponding normalized path loss term for all users can be equal to one, i.e., $L(d^k) = L(d) = 1$. In (8), $|\alpha_{i,j}^k| = \exp(x_{i,j}^k)$ represents the fading channel coefficient for the link between the i^{th} transmit and j^{th} receive aperture of k^{th} where x has Gaussian distribution, i.e., $N(\mu_x, \sigma_x^2)$ under log-normal turbulence assumption. Furthermore, in order to ensure that fading does not attenuate or amplify the average power, we consider $\mu_x = -\sigma_x^2$ [57]

2.3 Calculation of received SNR

Instantaneous received electrical SNR at the k^{th} user can be defined as [18, 28]

$$\gamma^k = \frac{\left(\mathbb{E} \left[r_{s_i,j}^k \right] - \mathbb{E} \left[r_{n_i,j}^k \right] \right)^2}{N_o} = \frac{R^2 T_b^2 P_{s,k}^2}{N_o} \quad (9)$$

Under the assumption of EGC, the optical power incident on the photodetector at j^{th} receive aperture of the k^{th} user can be expressed as [58]

$$P_{s,k}^k(j) = \left(\frac{P}{M_r} \right) \sum_{i=1}^{M_t} g_{i,j}^k = \frac{P_t}{M_t M_r} \sum_{i=1}^{M_t} |\alpha_{i,j}^k|^2 \quad (10)$$

where $P = P_t/M_t$ is average transmitted optical power per transmit aperture and P_t is the total transmit power. Therefore, we can rewrite the received electrical SNR at the k^{th} user as

$$\gamma^k = \frac{R^2 T_b^2 \left(\sum_{j=1}^{M_r} P_s^k(j) \right)^2}{N_o} = \frac{R^2 T_b^2 \left(\frac{P_t}{M_t M_r} \right)^2 \left(\sum_{j=1}^{M_r} \sum_{i=1}^{M_t} |\alpha_{i,j}^k|^2 \right)^2}{N_o} \quad (11)$$

Here, we substitute summation of log-normal r.v., e.i., $\sum_{j=1}^{M_r} \sum_{i=1}^{M_t} |\alpha_{i,j}^k|^2$ with approximated one denoted as $y = \exp(z)$ (for simplicity, we remove index k^{th} from rest of the equations due to iid distribution of the channel) where z is a Gaussian random

variable with a mean μ_z and a variance of σ_z^2 . We applied the well-known Fenton-Wilkinson method (Fenton-Wilkinson method is mostly accurate for small variance) to express mean and variance of z as following

$$\sigma_z^2 = \log \left(1 + \frac{e^{4\sigma_x^2} - 1}{M_t M_r} \right) \quad (12)$$

$$\mu_z = \log(M_t M_r) - \frac{1}{2}\sigma_y^2 \quad (13)$$

Hence, the overall received SNR at each user can be obtained as

$$\gamma = \frac{R^2 T_b^2 \left(\frac{P_t}{M_t M_r} \right)^2 y^2}{N_o} \quad (14)$$

2.4 Scheduling techniques

The advantage of scheduling methods based on CSI at the transmitter side is known to provide significant performance gain, i.e., higher throughput and lower outage probability in FSO system. The scheduling policies that maximizes system throughput transmits exclusively to the user that has the highest SNR at each given time slot. This types of scheduling polices which enhance the system performance gain can result in unfairness among users in a multiuser scheme. In order to improve the fairness, we need to assign similar number of slot times to all users during each round. Generally, there is a tradeoff between throughput and fairness so we can increase one at the cost of the other one.

2.4.1 Round Robin Scheduling

The simplest scheduling technique is the Round Robin (RR) method where slots are periodically assigned to active users in a predetermined order (in case of inactivity, RR method results in wasted bandwidth). In other words, the RR method treats users fairly in the sense that it allocates an equal share of time slots to each user, regardless of the channel condition (there is no need for CSI at the transmitter side) or whether there is data to be sent out to a particular user or not [59].

2.4.2 Opportunistic Round Robin method

Opportunistic Round Robin (ORR) scheduling technique is initially introduced by Kulkarni and Rosenberg in [60] to improve the short term fairness among users (where short term fairness refers to the time window on which the fairness is guaranteed). All users are assigned one of the time slots within a round. The user is assigned the time slots that maximizes the total throughput within a round. The proposed scheduling policy in [60] achieves a tradeoff by guaranteeing short term fairness while achieving high average system throughput. ORR scheduling method is further studied in [61, 62]. In [61, 62], ORR scheduling policy is employed in sequential rounds of N users based on CSI at the transmitter side. In detail, this scheduling method works as following, in the first time slot of a round, the user with the maximum SNR is selected, i.e. $\gamma^* = \max \{\gamma_1, \gamma_2, \dots, \gamma_N\}$ where N is the total number of users. In the second time slot, out of all users except selected best user in the first time slot compete and the user with the maximum SNR is allowed to receive data. In each of next time slots of a round, selected users in previous time slots are exempt from competition and the user with the maximum SNR out of the remaining users which has not yet been selected is scheduled to receive data. This procedure is continued until the last time slot, i.e. N^{th} time slot of the round when there is only one user left. Then, the procedure is restarted with all users again participating in the competition.

2.4.3 Select-max

Select-max scheduling protocol is originally devised in RF application to select among antennas in a spatial diversity combiner or in a multiuser system whereas multiuser diversity can be looked upon as spatial diversity, in which the spatial diversity combiner have been replaced by receivers [63]. Under the assumption of a frequency flat-fading channel model, the channel quality for each receiver can be characterized

by the instantaneous received SNR. Therefore, the receiver with the largest instantaneous SNR is selected for transmission across a particular time slot [52, 53]. The idea behind select-max technique is to employ the independent variation of multiuser channels and schedule the users with the best channel condition to transmit [52].

As such, multiuser FSO systems can also benefit from randomness of fading effects among the pairs of transmitter and receiver by means of select-max protocol. At any given time slot, the transmit node will probe all the receivers and schedule the receiver with the highest channel quality given as

$$k^* = \arg \max_k \{ \gamma_k \}, k = 1, \dots, N \quad (15)$$

where k^* denotes the best selected user with respected to the feedback SNR to the transmitter.

2.4.4 m^{th} Best Selection

Select-max technique is one of the most popular scheduling policy in corresponding to the selection of the best relay for cooperative FSO communications [26] or best user in the context of multiuser FSO systems [50, 54]. In some cases, it is possible that the conventional best user selection is not applicable due to some problems such as scheduling error, defective relay or load balancing [49, 50]. Hence, we have to select second best user or generally m^{th} best user for transmission. m^{th} best selection is initially introduced in [49] [49] to obtain performance degradation of RF cooperative communication systems by scheduling m^{th} best relay rather than the best one. In more detail, scheduling failure can be brought on by error in user selection caused by imperfect channel estimation. In practice, channel estimation needs to be carried out to determine the link quality and identify the relay/user which gives the highest instantaneous SNR (which is directly related to channel fading coefficient). As a result of imperfect channel estimation, the instantaneous SNR can be calculated with error and it might be possible to select another relay/user instead of the actual best

one. Another possible problem is defective relay/user. If the best relay/user, for some reasons, breaks down or malfunctions, we might need to resort to the second best or generally the m^{th} best relay/user. On the other hand, load balancing can be a concern in a multiuser system where multiple destinations are served through the same node [50].

2.5 Outage Probability Analysis

The outage probability is defined as the probability that the channel rate falls below the predefined value, R_0 and given as $P_{out}(R_0) = \Pr(\gamma < \gamma_{th})$ where γ_{th} shows the threshold SNR value [47]. Therefore the corresponding outage probability for each MIMO path between the transmitter and the user is given by

$$P(R_0) = \Pr\left(\frac{R^2 T_b^2 \left(\frac{P_t}{M_t M_r}\right)^2 y^2}{N_o} < \gamma_{th}\right) = F_y\left(\frac{M_t M_r}{P_\varepsilon}\right) \quad (16)$$

where $F_y(y)$ is the Cumulative Density Function (CDF) of the channel gain based on EGC at the receiver side. With respect to the definition of channel gain distribution between i^{th} aperture of the transmitter and j^{th} receive aperture of the k^{th} user given by

$$F_{g_{i,j}^k}(x) = 0.5 \operatorname{erfc}\left(-\frac{\log(x) - 2\mu_x}{\sqrt{8\sigma_x^2}}\right) \quad (17)$$

The CDF of the channel gain over each MIMO link can be expressed as

$$F_y\left(\frac{M_t M_r}{P_\varepsilon}\right) = 0.5 \operatorname{erfc}\left(\frac{\log\left(\frac{P_\varepsilon}{M_t M_r}\right) + \mu_z}{\sqrt{2\sigma_z^2}}\right) \quad (18)$$

where $P_\varepsilon = \sqrt{R^2 T_b^2 P_t^2 / (\gamma_{th} N_o)}$ denotes power margin [47]. The outage probability of prescribed scheduling methods can be presented over following sections.

2.5.1 Outage Probability Analysis of RR

Whereas in RR method, all users are subjected to iid fading distribution, all users experience the same probability of channel distributions. Thus, the total outage

probability of the system can be expressed as

$$P_{\text{out,RR}} = 0.5 \operatorname{erfc} \left(\frac{\log \left(\frac{P_\varepsilon}{M_t M_r} \right) + \mu_z}{\sqrt{2\sigma_z^2}} \right) \quad (19)$$

2.5.2 Outage Probability Analysis of ORR

With regard to ORR method, the CDF of the selected user channel gain can be stated as the average of the all competitor users in a round and given by [62]

$$F_{y^*}(y) = \frac{1}{N} \sum_{n=1}^N F_y^n(y) \quad (20)$$

where γ^* indicates the SNR of selected user within ORR method. Hence, the outage probability for FSO system based on ORR scheduling policy can be obtained as

$$P_{\text{out,ORR}} = \frac{1}{N} \sum_{n=1}^N \left(0.5 \operatorname{erfc} \left(\frac{\log \left(\frac{P_\varepsilon}{M_t M_r} \right) + \mu_z}{\sqrt{2\sigma_z^2}} \right) \right)^n \quad (21)$$

2.5.3 Outage Probability Analysis of select-max

The transmit node exploits the user with the largest SNR among all users. The outage probability of the system is presented as

$$P_{\text{out,select-max}} = \left(0.5 \operatorname{erfc} \left(\frac{\log \left(\frac{P_\varepsilon}{M_t M_r} \right) + \mu_z}{\sqrt{2\sigma_z^2}} \right) \right)^N \quad (22)$$

As it has been already explained, select-max technique (selecting the best user) can be considered as a special case of m^{th} best user selection which will be described in what follows.

2.5.4 Outage Probability Analysis of m^{th} Best Selection

As discussed in previous section, selecting suitable user can be performed by sorting all g_k values in a non-increasing order. Then, the m^{th} best user is selected among all N available ones. Using the notation of [64], the order statistics of sorted values are

denoted by $g_{1:N}, g_{2:N}, \dots, g_{N:N}$ where $g_{1:N} \geq g_{2:N} \geq \dots \geq g_{N:N}$ and $g_{m:N}$ indicates the m^{th} highest. The CDF of the m^{th} highest can be presented as [64]

$$F_{g_{m:N}}(y) = \sum_{j=1}^m \binom{N}{j-1} [F_y(y)]^{N-j+1} [1 - F_y(y)]^{j-1} \quad (23)$$

By substituting equation (18) in (23), an exact form of outage probability for the overall system based on m^{th} best user selection can be obtained as

$$P_{\text{out}} = \sum_{j=1}^m \binom{N}{j-1} \left[0.5 \operatorname{erfc} \left(\frac{\log \left(\frac{P_\varepsilon}{M_t M_r} \right) + \mu_z}{\sqrt{2\sigma_z^2}} \right) \right]^{N-j+1} \left[1 - 0.5 \operatorname{erfc} \left(\frac{\log \left(\frac{P_\varepsilon}{M_t M_r} \right) + \mu_z}{\sqrt{2\sigma_z^2}} \right) \right]^{j-1} \quad (24)$$

Through the achieved result in (24), if we consider $m = 1$ (best user selection), we will obtain the similar result same as select-max technique.

2.5.5 Numerical Results and Discussions

In this section, we verify the accuracy of derived outage probability through Monte Carlo simulations and present the outage probability through predescribed scheduling policies. We assume an FSO system with $\lambda = 1550$ nm under clear weather conditions with a visibility of 10 km. The distance between the source and the users is assumed to be 3 km. The total number of users is $N = 8$. Furthermore, we consider an atmospheric attenuation of 0.42 dB/km (i.e., $\tau \approx 0.1$) and refraction structure parameter of $C_n^2 = 1 \times 10^{-14} \text{m}^{-2/3}$.

In Fig.2, we illustrate the outage performance versus power margin (P_ε) of FSO system under the assumption which all users are located equidistantly from the transmitter. As it has been mentioned above there are totally $N = 8$ users. Both the transmitter and users are equipped with $M_r = 2$ and $M_t = 2$ transmit and receive apertures, respectively. As a benchmark, we further include the case of SISO scenario where each user and the transmitter employ only one transmit and receive aperture,

respectively. The analytical results are provided based on the derived outage probability expressions for different scheduling techniques. In addition to the obtained results, we can observe accurate match for the approximation technique used over summation of log-normal random variables, particularly in low power margin regime. As it has been illustrated in Fig. 2, for a target outage probability of 10^{-6} , we need $P_\epsilon = 2.1$ dB in MIMO scheme for select-max method which outperforms SISO scenario by 2.3 dB. In case of selecting second best user instead of the best one, it requires 2.7 dB and 5.5 dB for MIMO and SISO scenarios, respectively. ORR scheduling technique requires 8 dB in MIMO scheme which is increased by 15.5 dB for SISO scenario. In RR method, the target outage probability acquires 9.3 dB and 17.3 dB in MIMO and SISO, respectively. Although, the target outage probability can be achieved at high power margin based on RR scheduling technique, it provides the best fairness among the rest of the techniques, specifically, for the transmissions which can tolerate high latency.

Fig.3 depicts the outage performance of MU-MIMO FSO system under the assumption of $P_\epsilon = 4$ dB and $M_t = 2$ and $M_r = 2$ with respect to the number of users. As it has been illustrated in Fig. 3, the outage probability of m^{th} best selection decreases dramatically compared to ORR and RR scheduling techniques. As it can be understood, selecting 1st, 2nd and 3rd best user have the same trend and slope by increasing the number of users.

As it is clear, the outage probability of RR technique does not change by raising the users number. On the other hand, opportunistic scheduling policies (select-max, m^{th} best user selection and ORR) show better performance results at high number of users. For instance, 1st, 2nd and 3rd best user selection respectively achieve to the target outage probability of 10^{-6} at $N=4, 5$ and 7 . While, ORR reaches to the same outage probability at much more large number of users.

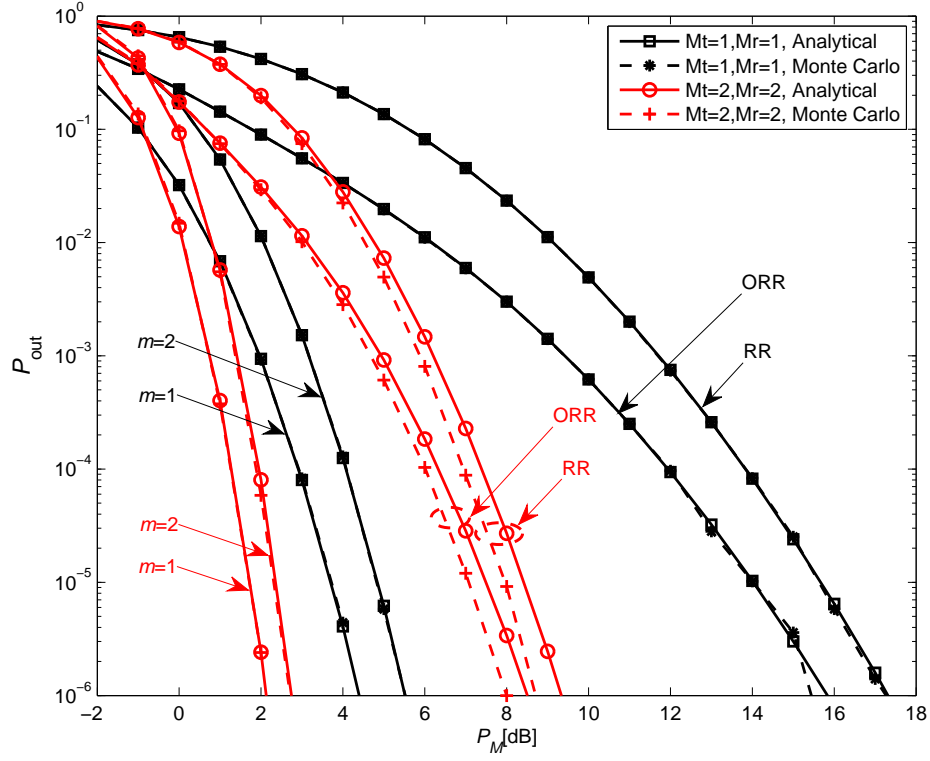


Figure 2: Outage performance of MU-MIMO FSO system with 1st (select-max), 2nd best user selection, ORR and RR scheduling policies. Assuming $N = 8$ and $M_t = 2$ and $M_r = 2$. As a benchmark, the performance of multiuser SISO scenario ($N = 8$ and $M_t = 1$ and $M_r = 1$) is included.

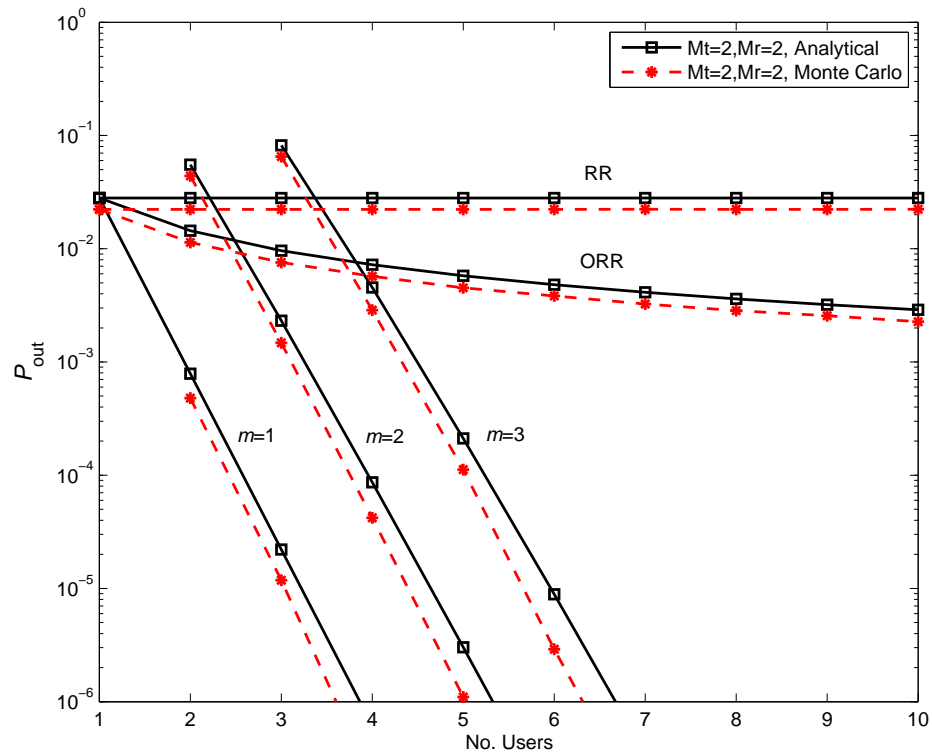


Figure 3: Outage performance of MU-MIMO FSO system with 1st (select-max), 2nd, ORR and RR scheduling policies with respect to the number of users is presented, assuming $N = 8$ and $M_t = 2$ and $M_r = 2$.

CHAPTER III

OUTAGE PROBABILITY ANALYSIS OF MULTIHOP PARALLEL FSO SYSTEMS

3.1 Introduction

In this chapter, we extend our multiuser scenario to a more general case in the form of cooperative FSO communication. Specifically, we investigate the performance of multiuser FSO systems with parallel multihop relaying and use m^{th} best path selection (m-BPS) which can be considered as an extension of m^{th} best user selection discussed in the previous chapter. We consider an FSO communication system which employs M parallel relaying paths each of which consists of N decode-and-forward relays. We assume the deployment of m-BPS protocol. In this protocol, data is transmitted through the m^{th} ($m \geq 2$) best path towards the destination since the best path (i.e., $m = 1$) might not be available due to scheduling or load balancing issues. Under the assumption of log-normal turbulence channels, we derive a closed-form outage probability expression for the FSO communication system with m-BPS protocol and demonstrate that a diversity gain of $(M - m + 1)(N + 1)^{11/6}$ is available.

3.2 System Model

The system model under consideration is illustrated in Fig. 4. We assume a relay-assisted FSO communication system where the transmission between the source (S) and the destination node (D) is facilitated by means of M parallel relaying paths. Each of these paths consists of N decode-and-forward (DF) relays which are located non-equidistantly from each other. In Fig.4, $R_{k,i}$ denotes the $i^{\text{th}} \in \{1, \dots, N\}$ relay node positioned on the $k^{\text{th}} \in \{1, \dots, M\}$ path and each node is equipped with single

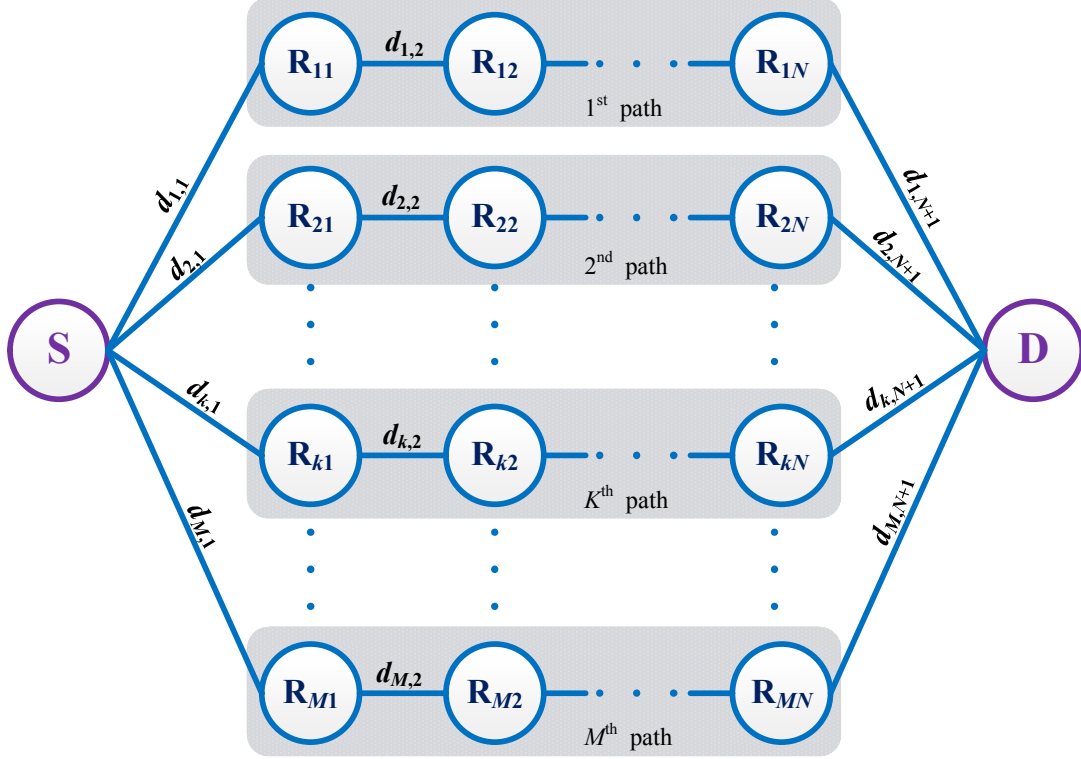


Figure 4: FSO system with M paths each of which consists of N relay nodes.

transmit/receive aperture. In our system, data is transmitted through a selected path towards the destination.

For the purpose of path selection, channel gains are monitored and fed back to the source. Let $g_{k,i}$ represent the channel gain of the link between $(i - 1)^{\text{th}}$ and i^{th} nodes in the k^{th} path. The source first determines the weakest link (i.e., lowest channel gain) in each path which is given by

$$g_{k,min} = \min\{g_{k,1}, g_{k,2}, \dots, g_{k,N+1}\}, k = 1, \dots, M \quad (25)$$

Then, it sorts all $g_{k,min}$ values in a non-increasing order and chooses the m^{th} best path among M paths. As mentioned earlier, the motivation for choosing the m^{th} best one rather than the best one relies on the fact that the best relay might be unavailable due to some scheduling or load balancing issues.

We consider IM/DD and BPPM modulation technique in our system. After

optical-to-electrical conversion, the relay decodes the signal in electrical domain, modulates it using BPPM, and retransmits it to the next relay or to the destination in the last hop.

Let $r_{s_k,i}$ and $r_{n_k,i}$, $i = 1, \dots, N$, respectively, denote the received electrical signals over the signal and non-signal slots of BPPM pulse for the relay node $R_{k,i}$ [47]. They are expressed as

$$r_{s_k,i} = \Gamma T_b (P g_{k,i} + P_b) + n_{s_k,i} \quad (26)$$

$$r_{n_k,i} = \Gamma T_b P_b + n_{n_k,i} \quad (27)$$

where Γ represents the responsivity of the photodetector and T_b is the duration of signal/non-signal slots in (26) and (27). P indicates the average transmitted optical power which is related to the system power budget (P_t) by $P = P_t/(N + 1)$. P_b represents the background power on the photodetector. $n_{s_k,i}$ and $n_{n_k,i}$ denote the AWGN terms for the signal and non-signal slots which are modeled with zero mean and variance of $\sigma_n^2 = N_0/2$.

The channel gain $g_{k,i}$ is defined as [47]

$$g_{k,i} = L(d_{k,i}) |\alpha_{k,i}|^2 \quad (28)$$

where $L(d_{k,i}) = l(d_{k,i})/l(d_{k,N+1})$ denotes the normalized path loss with respect to the distance of the direct path between the source and destination, i.e., $d_{k,N+1}$, $k = 1, \dots, M$ and $i = 1, \dots, N + 1$. The path loss ratio of an FSO link is given by $l(d) = e^{-\tau d} A_{TX} A_{RX}/(\lambda d)^2$ where A_{TX} and A_{RX} are transmit and receive aperture area, respectively and τ is the attenuation coefficient determined by the exponential Beers-Lambert law.

In (28), $|\alpha_{k,i}| = \exp(x_{k,i})$ represents the fading channel coefficient for the link between $(i - 1)^{\text{th}}$ and i^{th} nodes on the k^{th} path where $x_{k,i}$ has Gaussian distribution, i.e., $N(\mu_{x_{k,i}}, \sigma_{x_{k,i}}^2)$ under log-normal turbulence assumption. The channel coefficients are assumed to be independent and non-identical distributed (inid). Furthermore,

in order to ensure that fading does not attenuate or amplify the average power, we consider $\mu_{x_{k,i}} = -\sigma_{x_{k,i}}^2$ [57]. Using the Rytov approximation for weak turbulence, the log-amplitude variance, $\sigma_{x_{k,i}}^2$ is given by $\sigma_{x_{k,i}}^2(d_{k,i}) = 0.124C_n^2 k^{7/6} d_{k,i}^{11/6}$ where C_n^2 denotes the index of refraction structure parameter, k is the optical wave number and $d_{k,i}$ is distance of the i^{th} link on the k^{th} path.

3.3 Outage Probability Analysis

The outage probability is defined as the probability that the channel rate falls below the targeted value, R_0 and given as $P_{\text{out}}(R_0) = \Pr(\gamma < \gamma_{th})$ where γ_{th} shows the threshold SNR value. Instantaneous electrical SNR for the link between the $(i-1)^{\text{th}}$ and the i^{th} nodes on the k^{th} path is given by [47]

$$\gamma_{k,i} = \frac{\Gamma^2 T_b^2 P_t^2 g_{k,i}^2}{N_o(N+1)^2} \quad (29)$$

Therefore the corresponding outage probability is obtained as

$$P_{k,i}(R_0) = \Pr\left(g_{k,i} < \frac{N+1}{P_\varepsilon}\right) = F_{g_{k,i}}\left(\frac{N+1}{P_\varepsilon}\right) \quad (30)$$

where $P_\varepsilon = \sqrt{\Gamma^2 T_b^2 P_t^2 / (\gamma_{th} N_o)}$ denotes power margin [47] and $F_{g_{k,i}}$ is the CDF of the random variable $g_{k,i}$. The CDF of the minimum channel gain over the k^{th} path, i.e., $g_{k,min}$, is given by

$$F_{g_{k,min}}(x) = 1 - \prod_{i=1}^{N+1} (1 - F_{g_{k,i}}(x)) \quad (31)$$

where $F_{g_{k,i}}(x) = 0.5 \operatorname{erfc}\left(-(\ln(x/L(d_{k,i})) - 2\mu_{x_{k,i}}) / \sqrt{8\sigma_{x_{k,i}}^2})\right)$ with $\operatorname{erfc}(\cdot)$ denoting the complementary error function. Thus, the corresponding outage probability is obtained as

$$P_{k,min}(R_0) = 1 - \prod_{i=1}^{N+1} \left[1 - \frac{1}{2} \operatorname{erfc}\left(\frac{\ln\left(\frac{L(d_{k,i})P_\varepsilon e^{2\mu_{x_{k,i}}}}{N+1}\right)}{\sqrt{8\sigma_{x_{k,i}}^2}}\right) \right] \quad (32)$$

As discussed in chapter 2, in order to select the suitable path for transmission, all $g_{k,min}$ values are sorted in a non-increasing order. Then, the m^{th} best one is selected

among all M paths. Following the notation of [65], the order statistics of sorted $g_{k,min}$ variables are denoted by $g_{1:M}, g_{2:M}, \dots, g_{M:M}$ ($g_{1:M} \geq g_{2:M} \geq \dots \geq g_{M:M}$) where $g_{m:M}$ indicates the m^{th} highest $g_{k,min}$. Using order statistics, [65], we obtain the outage probability as

$$P_{\text{out}} = \sum_{j=1}^m \frac{1}{(j-1)!(M-j+1)!} \text{Per}\mathbf{Z} \quad (33)$$

In (33), $\text{Per}\mathbf{Z}$ denotes the permanent of matrix \mathbf{Z} which is defined as

$$\mathbf{Z} = \begin{bmatrix} P_{1,min} & P_{2,min} & \cdots & P_{M,min} \\ 1 - P_{1,min} & 1 - P_{2,min} & \cdots & 1 - P_{M,min} \end{bmatrix} \begin{matrix} \} M - j + 1 \\ \} j - 1 \end{matrix} \quad (34)$$

where the matrix elements $P_{k,min}$ have been already defined in (32). Here, the notation $\cdot\}M-j+1$ indicates that the first row is repeated $M-j+1$ times. Similarly, the second row is repeated $j-1$ times.

As a special case, we also consider a scenario where all relay nodes are placed equidistant from each other. In this case, we have $d_{k,i} = d$, $\mu_{x_{k,i}} = \mu_x$, $\sigma_{x_{k,i}}^2 = \sigma_x^2$, $\forall i \in \{1, \dots, N+1\}$ and $\forall k \in \{1, \dots, M\}$. Using properties of permanent operation [65], it can be shown that (33) reduces to

$$P_{\text{out}} = \sum_{j=1}^m \binom{M}{j-1} \left[1 - \left[1 - \frac{1}{2} \text{erfc} \left(\frac{\ln \left(\frac{L(d)P_\epsilon e^{2\mu_x}}{N+1} \right)}{\sqrt{8\sigma_x^2}} \right) \right]^{(N+1)} \right]^{(M-j+1)} \\ \times \left[1 - \frac{1}{2} \text{erfc} \left(\frac{\ln \left(\frac{L(d)P_\epsilon e^{2\mu_x}}{N+1} \right)}{\sqrt{8\sigma_x^2}} \right) \right]^{(N+1)(j-1)} \quad (35)$$

where $L(d) = \exp(\tau N d_{k,N+1} / (N+1)) (N+1)^2$.

3.4 Diversity Order Analysis

Diversity order is conventionally defined as the negative asymptotic slope of outage probability versus SNR. This conventional definition results in infinity over log-normal channels and does not provide any useful information. Instead, we employ so-called

Relative Diversity Order (RDO) which has been introduced in [66] as

$$\text{RDO}(P_\varepsilon) = \frac{\partial \ln P_{\text{out}} / \partial \ln P_\varepsilon}{\partial \ln P_{\text{out,sd}} / \partial \ln P_\varepsilon} \quad (36)$$

where $P_{\text{out,sd}}$ indicates the outage probability of the direct path between the source and the destination. The Asymptotic RDO (ARDO) can be further defined as $\text{ARDO} = \lim_{P_\varepsilon \rightarrow \infty} \text{RDO}(P_\varepsilon)$ [66].

As it will be later revealed from numerical results, the best performance is achieved when the relays on each path are located equidistant from each other. In the following, we carry out the diversity analysis for this special case. Using the limiting expressions $\lim_{x \rightarrow \infty} \text{erfc}(x) \approx 0$, $\lim_{x \rightarrow 0} (1+x)^n \approx 1+nx$ in (35) and, after some mathematical manipulations of the resulting expressions, we can write (35) as

$$P_{\text{out}} \approx \binom{M}{m-1} \left[\frac{N+1}{2} \text{erfc} \left(\frac{\ln \left(\frac{L(d)P_\varepsilon e^{2\mu x}}{N+1} \right)}{\sqrt{8\sigma_x^2}} \right) \right]^{(M-m+1)} \quad (37)$$

By substituting (37) in (36), using $\text{erfc}(x) < e^{-x^2}$ for $x \geq 0$ [67] and performing the differentiation, we obtain the ARDO as

$$\text{ARDO} = \lim_{P_\varepsilon \rightarrow \infty} \frac{\frac{M-m+1}{4\sigma_x^2} \ln \left(\frac{L(d)P_\varepsilon e^{2\mu x}}{N+1} \right)}{\frac{1}{4\sigma_{sd}^2} \ln(P_\varepsilon e^{2\mu_{sd}})} \quad (38)$$

where μ_{sd} and σ_{sd}^2 are, respectively, the mean and variance of channel coefficient for the direct path between the source and the destination nodes. Taking the limit in (38) and replacing the definitions of σ_{sd}^2 and σ_x^2 based on the Rytov formula, we can express the ARDO as

$$\text{ARDO} = (M - m + 1)(N + 1)^{\frac{11}{6}} \quad (39)$$

Eq. (39) can be seen as a generalization of the results in [68]. If we insert $M = m = 1$, we obtain $(N + 1)^{11/6}$ which coincides Eq. (36) of [68] for the case of single-path serial DF relaying.

3.5 Numerical Results and Discussions

In this section, we verify the accuracy of derived outage probability through Monte Carlo simulations and present the diversity gains available through relaying and path selection. We assume an FSO system with $\lambda=1550$ nm under clear weather conditions with a visibility of 10 km. The distance between the source and the destination is assumed to be 4 km. Furthermore, we consider an atmospheric attenuation of 0.42 dB/km (i.e., $\tau \approx 0.1$) and refraction structure parameter of $C_n^2 = 1 \times 10^{-14} \text{m}^{-2/3}$.

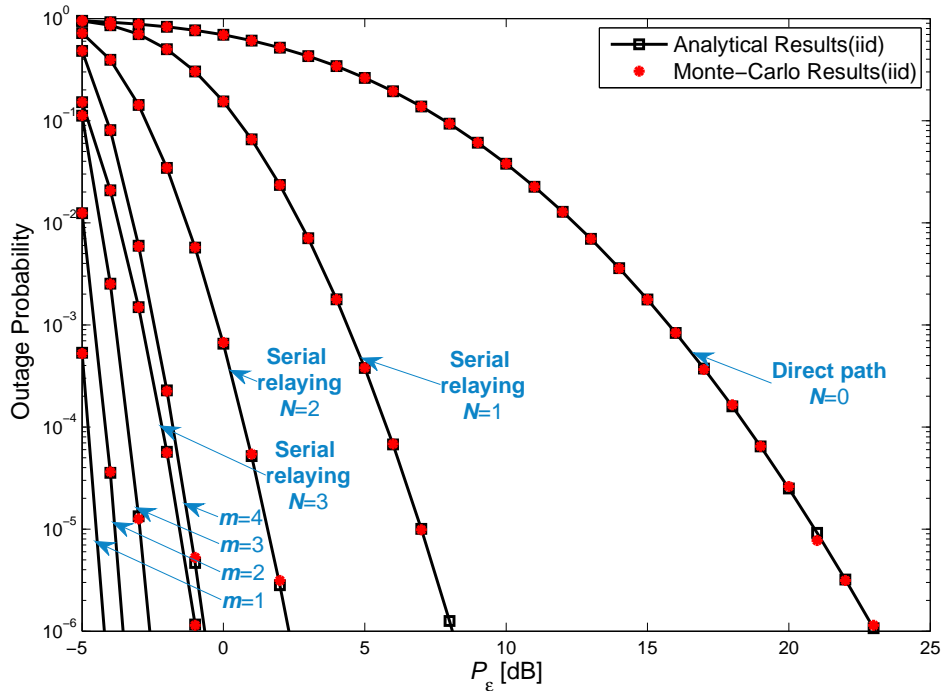


Figure 5: Outage performance of FSO system with 1st, 2nd, 3rd and 4th best path selection assuming $M = 4$ and $N = 3$. As a benchmark, the performance of serial relaying path ($M = 1$ and $N = 3, 2, 1$) along with direct path communication ($M = 1$ and $N = 0$) are included.

In Fig.5, we illustrate the outage performance versus power margin (P_ϵ) of FSO system under the assumption that the relays are located equidistantly on each path. In this system, there are four parallel paths ($M = 4$) and each path includes 3 relays ($N = 3$). As benchmarks, we further include the case of direct transmission (i.e., no

Table 1: FSO system configuration

Path No	$d_{k,1}$	$d_{k,2}$	$d_{k,3}$	$d_{k,4}$	S to D
$k=1$	$d_{sd}/8$	$2d_{sd}/8$	$3d_{sd}/8$	$2d_{sd}/8$	d_{sd}
$k=2$	$d_{sd}/8$	$3d_{sd}/8$	$2d_{sd}/8$	$2d_{sd}/8$	d_{sd}
$k=3$	$d_{sd}/8$	$2d_{sd}/8$	$2d_{sd}/8$	$3d_{sd}/8$	d_{sd}
$k=4$	$3d_{sd}/8$	$d_{sd}/8$	$2d_{sd}/8$	$2d_{sd}/8$	d_{sd}

relays) and serial relaying (i.e., no parallel paths) with $N = 1, 2, 3$. The analytical results are provided based on the derived expression in (35). The obtained results provide perfect match to simulation results confirming the accuracy of derivation. To achieve a targeted outage probability of 10^{-6} , we need $P_\epsilon = 23$ dB for the case of direct path between the source and destination. For the FSO system with m-BPS protocol (assuming $M=4$ and $N=3$), the required power margin decreases to $P_\epsilon = -4.2$ dB, if the best path is selected. If the best path is not available, we can choose the second best one, i.e., $m = 2$, which requires $P_\epsilon = -3.5$ dB. This indicates a performance improvement over the direct transmission by $P_\epsilon = 26.5$ dB. The performance gains over serial relaying cases with $N=1, 2, 3$ are observed to be respectively $P_\epsilon = 8.1$ dB, and $P_\epsilon = 2.3$ dB and $P_\epsilon = -0.97$ dB. Even, with the choice of the third best one, i.e., $m = 3$, we are still able to outperform the serial relaying case with $N = 3$ by a difference of 1.6 dB.

Fig.6 depicts the outage performance of FSO system for $M = 4$ and $N = 3$ for a specific scenario (see Table I) where relays are placed non-equidistantly from each other. As a benchmark, we also include the performance where all relays are placed equidistantly from each other (labeled as iid in the figure). The analytical results are provided based on (33) obtained within iid assumption. Similar to Fig. 5, we observe a perfect match between analytical and simulation results. It is also observed that iid scenario provides a better performance. For example, through 1st, 2nd, 3rd and 4th best path selection, outage performance are improved by $P_\epsilon = 4.3$ dB,

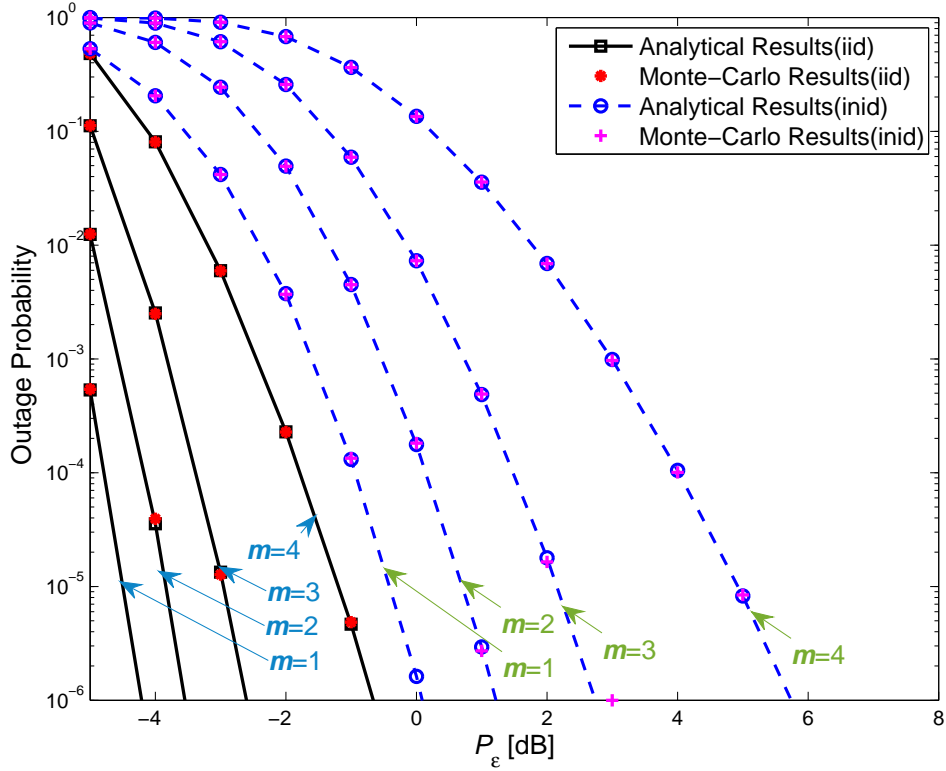


Figure 6: Outage performance of iid and inid FSO system with 1st, 2nd, 3rd and 4th best path selection assuming $M=4$ and $N=3$.

$P_\epsilon = 4.8$ dB, $P_\epsilon = 5.3$ dB and $P_\epsilon = 6.4$ dB with respect to the inid scenario in Table I. This observation is also in line with [68] which addresses the choice of optimized relay location in serial FSO relaying and concludes that relays should be located equidistant from each other.

In Fig. 10, we present the diversity order results. We assume $M=4$, $N=3$ and plot the RDO results for $m=1, 2, 3, 4$ based on (36). Our results show that RDO converges to 51, 38.3, 25.4 and 12.7, respectively, in high SNR regime verifying the derived ARDO expression in (39). It is also observed that m-BPS protocol with $m=4$ (i.e., worst case scenario) achieves the same diversity gain with that of (single path) serial relaying.

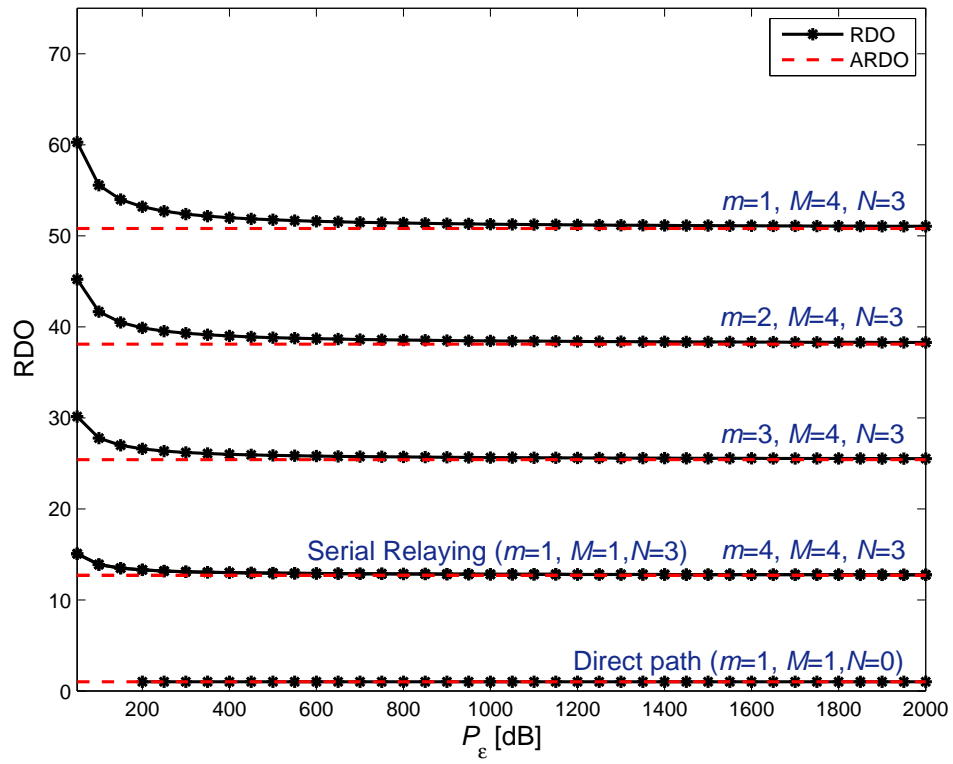


Figure 7: RDO and ARDO comparison of FSO system by m-BPS.

CHAPTER IV

OUTAGE CAPACITY ANALYSIS OF MULTIUSER FSO SYSTEM

4.1 Introduction

There are two main information theoretic metrics of capacity. These are ergodic capacity and outage capacity. The former is defined as the expectation of instantaneous capacity while the latter is the largest rate of reliable communication at a certain outage probability. The ergodic capacity is mostly employed in fast fading channels where it is possible to code over many channel gains and achieve reliable rates up to the ergodic capacity which is defined as the average maximum mutual information per second. In order to utilize the ergodic capacity metric, it is necessary that the codeword extent over at least several atmospheric channel coherence times which makes it feasible to code across both deep and shallow fade channel gains.

Unlike the fast fading channel model, due to the delay constraints and coherence time within slow fading channels which prevent averaging over deep and shallow channel gains, it is possible that the fading becomes so severe that the instantaneous capacity is below any desired rate. As a result, a more realistic measure of capacity is the probability that the channel can support a target rate. Since, slow fading channels become more appropriate model to describe optical communications channels as data rate increases [8], our goal in this chapter is to derive outage capacity for a multiuser FSO system.

Outage capacity has been investigated in RF literature. In [69], authors studied outage capacity in cooperative communications with modified amplified and forward protocol, specifically in low SNR and low outage probability regime. In [70], the

outage capacity of a multiuser MIMO system has been studied under the assumption of MRC.

Outage capacity has been recently explored in the context of FSO communications. In [71], the authors investigated the outage capacity of FSO using MIMO scheme over log-normal fading model. They studied outage capacity in high and low SNR regime. In [42], the authors studied the impact of aperture averaging on the system performance through outage capacity, particularly considering two cases of background and thermal noise-limited receivers over Gamma-Gamma channel model. Outage capacity has been obtained for MISO FSO system in [72]. The channel model was assumed to be employed under the consideration of both atmospheric and misalignment fading over log-normal channel model and last but not least, the outage capacity of coherent FSO system over log-normal along with Gaussian phase fluctuations and local oscillator shot noise has been studied in [8]. To the best of our knowledge, no one has studied the outage capacity and throughput of multiuser FSO systems so far. Thus, in this chapter, we investigate the outage capacity of multiuser FSO system in both iid and inid scenarios under the assumption of log-normal channel model.

4.2 System Model

The system model under consideration is illustrated in Fig. 8. We assume a multiuser FSO system with N users. In the proposed scheme, the transmitter is equipped with multiple apertures while each user has only one receive aperture. The users are located non-equidistantly from the transmitter node. Furthermore, it is assumed that atmospheric channels are modeled through log-normal distribution and also, the scheduler at the transmit side employs select-max technique.

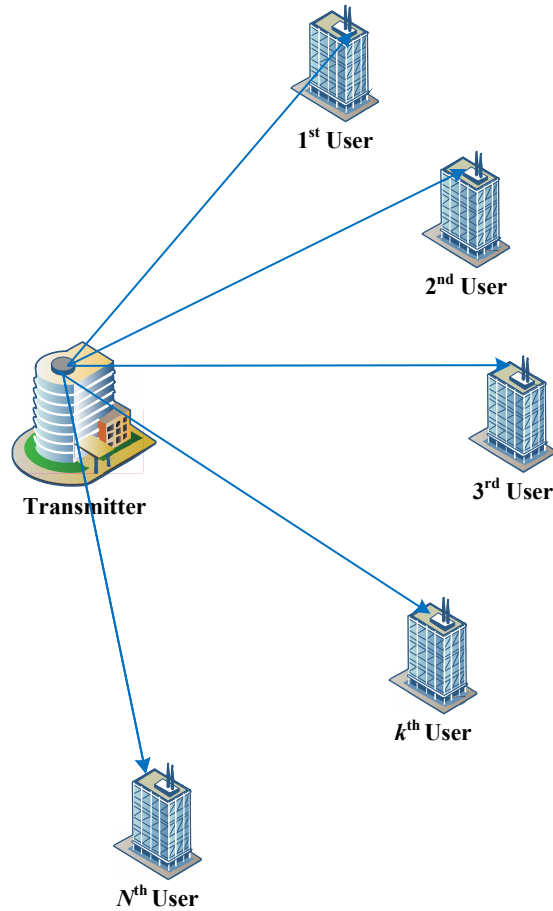


Figure 8: FMultiuser SISO FSO system with one transmitter and N users.

4.3 Outage Capacity Analysis

Channel capacity, C , is the maximal data rate at which the information can be transmitted over the channel with arbitrarily small probability of error. In the case of quasi-static channels, (i.e., the intensity of the optical signal follows slow fading statistics), it is possible that the transmitter encodes data at a rate, R , but if the channel realization, i.e. α fails to support the given rate, R , we will have $C = \log_2(1 + SNR) < R$ at the receiver side where the outage occurs. In this case, transmitted codewords cannot be decoded correctly at the receiver with arbitrarily small probability of error [73,74]. Thus, the capacity of FSO channel can be described

by means of outage probability and the corresponding outage capacity. Let γ_{th} denote SNR that is required to support a rate R_{th} over an AWGN channel. As we have already explained in previous chapters, since the channel capacity is monotonically increasing with transmitted power for a given channel state, the outage event can be expressed in terms of the SNR as $P_{out}(R_{th}) = \Pr(\gamma < \gamma_{th})$.

The outage capacity, i.e. C_ε shows the largest rate of transmission, i.e., R_{th} such that the outage probability is less than ε . This result can be presented in terms of the complementary cumulative distribution function (CCDF) of the SNR, as $P_{out}(R_{th}) = 1 - F_c(\gamma_{th})$. By solving $P_{out}(R_{th}) = \varepsilon$ with respect to SNR term, i.e. $F_c(\gamma_{th}) = 1 - \varepsilon$, the SNR can be expressed as $\gamma_{th} = F_c^{-1}(1 - \varepsilon)$. Finally, by definition, the ε -outage capacity is obtained as [8, 51, 74]

$$C_\varepsilon = B \log_2(1 + \gamma_{th}) = B \log_2[1 + F_c^{-1}(1 - \varepsilon)] \quad (40)$$

Alternatively, it is reasonable to consider a certain percentage of outage, i.e., ε , and try to achieve rate R for the rest of the transmission period. The maximum rate that can be obtained under the consideration of fixed outage probability, i.e. ε , is defined as ε percent outage capacity given as [75, 76]

$$C_\varepsilon = \max \{R: P_{out}(R) \leq \varepsilon\} \quad (41)$$

we can describe the outage capacity as the guaranteed capacity for $(1 - \varepsilon)\%$ of channel gain [77]. Hence, we can express outage throughput as the maximum successful transmission to the destination as [78]

$$T = (1 - \varepsilon) \max_\varepsilon \{R: P_{out}(R) \leq \varepsilon\} \quad (42)$$

Here, we derive outage capacity and consequently outage throughput of multiuser SISO FSO system as described in (41) and (42). The outage probability can be shown as $P_{out}(R) = \Pr(\gamma < 2^{C_\varepsilon} - 1)$. Instantaneous electrical SNR for the optical

link of proposed system between the transmitter and the i^{th} receiver is given by $\gamma_i = \Gamma^2 T_b^2 P_t^2 g_i^2 / N_o$ [47]. The instantaneous SNR is further described as

$$\gamma_i = \bar{\gamma} L(d_i)^2 |\alpha_i|^4 \quad (43)$$

where $\bar{\gamma} = \Gamma^2 T_b^2 P_t^2 / N_o$ denotes average SNR. Therefore the corresponding outage probability for each link from the transmitter to i^{th} receiver is given by

$$P_{out,i}(R) = \Pr \left(|\alpha_i|^4 < \frac{2^{C_\varepsilon} - 1}{\bar{\gamma} L(d_i)^2} \right) = F_{|\alpha_i|^4} \left(\frac{2^{C_\varepsilon} - 1}{\bar{\gamma} L(d_i)^2} \right) \quad (44)$$

$F_{|\alpha_i|^4}(x)$ is the CDF of the random variable $|\alpha_i|^4$. The CDF of $|\alpha_i|^4$ is given by $F_{|\alpha_i|^4}(x) = 0.5 \operatorname{erfc} \left(-(\ln(x) - 4\mu_{x_i}) / \sqrt{32\sigma_{x_i}^2} \right)$. Consequently, the outage probability can be further expressed as

$$P_{out,i}(R) = 0.5 \operatorname{erfc} \left(\frac{1}{\sqrt{32\sigma_{x_i}^2}} \ln \left(\frac{\bar{\gamma} L(d_i)^2 e^{4\mu_{x_i}}}{2^{C_\varepsilon} - 1} \right) \right) \quad (45)$$

Under the assumption of select-max scheduling protocol for the considered Multiuser FSO system, the total outage probability of the system can be demonstrated as

$$P_{out}(R) = \varepsilon = \prod_{i=1}^N \left[0.5 \operatorname{erfc} \left(\frac{1}{\sqrt{32\sigma_{x_i}^2}} \ln \left(\frac{\bar{\gamma} L(d_i)^2 e^{4\mu_{x_i}}}{2^{C_\varepsilon} - 1} \right) \right) \right] \quad (46)$$

In what follows, we will investigate the outage capacity and throughput in two cases of independent non-identical and identical distributions.

4.3.1 Independent Non Identical Distribution

The outage capacity can be obtained through (46). Since, it is difficult to obtain a closed-form solution because of containing nonlinear function, numerical methods are used to find outage capacity from (46). For instance, we have used the *fsolve* function of MATLAB to calculate C_ε .

Also, by means of a strict upper chernoff bound given as $\operatorname{erfc}(x) \leq 2e^{-x^2}$ for $x \geq 0$ [67], it is possible to obtain a lower bound of outage capacity. Eq. (46) can be

written by using chernoff bound as

$$\varepsilon = \prod_{i=1}^N \left[\exp \left(-\frac{1}{32\sigma_{x_i}^2} \left(\ln \left(\frac{\bar{\gamma}L(d_i)^2 e^{4\mu_{x_i}}}{2^{C_\varepsilon} - 1} \right) \right)^2 \right) \right] \quad (47)$$

After applying logarithmic function on (47), it can be expressed as

$$\ln(\varepsilon) = \sum_{i=1}^N \frac{-1}{32\sigma_{x_i}^2} \left[\ln(\bar{\gamma}L(d_i)^2 e^{4\mu_{x_i}}) - \ln(2^{C_\varepsilon} - 1) \right]^2 \quad (48)$$

Then, by employing the Quadratic equation, i.e., $ax^2 + bx + c = 0$ and assuming $x = \ln(2^{C_\varepsilon} - 1)$, we could obtain the outage capacity under the following coefficients assumption as

$$a = \sum_{i=1}^N \frac{-1}{32\sigma_{x_i}^2} \quad (49)$$

$$b = \sum_{i=1}^N \frac{\ln(\bar{\gamma}L(d_i)^2 e^{4\mu_{x_i}})}{16\sigma_{x_i}^2} \quad (50)$$

$$c = \sum_{i=1}^N \frac{-(\ln(\bar{\gamma}L(d_i)^2 e^{4\mu_{x_i}}))^2}{32\sigma_{x_i}^2} - \ln(\varepsilon) \quad (51)$$

Finally by substituting obtained x in $C_\varepsilon = \log_2(1 + e^x)$ the outage capacity can be calculated. The outage throughput is simply obtained by the following expression given as

$$T_\varepsilon = (1 - \varepsilon) C_\varepsilon \quad (52)$$

4.3.2 Independent Identical Distribution

For the case of iid where all receivers are placed equidistantly from the transmitter, we have $\sigma_{x_i}^2 = \sigma_x^2$ and $\mu_{x_i} = \mu_x$ for $\forall i \in \{1, \dots, N\}$. Furthermore, from the equal distance assumption, we can conclude $L(d_i) = 1$ for $\forall i \in \{1, \dots, N\}$. The outage capacity can be obtained by the following manipulations. Firstly, the total outage capacity of the system is given as

$$P_{out}(R) = \varepsilon = \left[0.5 \operatorname{erfc} \left(\frac{1}{\sqrt{32\sigma_x^2}} \ln \left(\frac{\bar{\gamma}e^{4\mu_x}}{2^{C_\varepsilon} - 1} \right) \right) \right]^N \quad (53)$$

Then, after some mathematical simplification and implementing Inverse Complementary Error Function (erfcinv), we have the following expression

$$\ln \left(\frac{\bar{\gamma} e^{4\mu_x}}{2C_\varepsilon - 1} \right) = \sqrt{32\sigma_x^2} \text{erfcinv} \left(2 \sqrt[N]{\varepsilon} \right) \quad (54)$$

Finally, the outage capacity and throughput can be respectively presented as

$$C_\varepsilon = \log_2 \left(1 + \bar{\gamma} e^{4\mu_x} \exp \left\{ -\sqrt{32\sigma_x^2} \text{erfcinv} \left(2 \sqrt[N]{\varepsilon} \right) \right\} \right) \quad (55)$$

$$T_\varepsilon = (1 - \varepsilon) \log_2 \left(1 + \bar{\gamma} e^{4\mu_x} \exp \left\{ -\sqrt{32\sigma_x^2} \text{erfcinv} \left(2 \sqrt[N]{\varepsilon} \right) \right\} \right) \quad (56)$$

At high SNR regime, (55) is simplified by employing $\log(1+x) \approx \log(x)$ for large value of x given by

$$C_\varepsilon = \log_2(\bar{\gamma}) + \frac{1}{\ln 2} \left(4\mu_x - \sqrt{32\sigma_x^2} \text{erfcinv} \left(2 \sqrt[N]{\varepsilon} \right) \right) \quad (57)$$

where by assuming $C_{\text{AWGN}} \approx \log_2(\bar{\gamma})$, (55) and (56) can be rewritten through a constant difference regardless of the SNR as

$$C_\varepsilon = C_{\text{AWGN}} + \frac{1}{\ln 2} \left(4\mu_x - \sqrt{32\sigma_x^2} \text{erfcinv} \left(2 \sqrt[N]{\varepsilon} \right) \right) \quad (58)$$

$$T_\varepsilon = (1 - \varepsilon) \left[C_{\text{AWGN}} + \frac{1}{\ln 2} \left(4\mu_x - \sqrt{32\sigma_x^2} \text{erfcinv} \left(2 \sqrt[N]{\varepsilon} \right) \right) \right] \quad (59)$$

Since, there is no known inverse of the erfc(.) function, we represent the erfc(.) function by a strict upper chernoff bound given as $\text{erfc}(x) \leq 2e^{-x^2}$ for $x \geq 0$ [67] and as a result lower bound of C_ε under the assumption of iid scheme can be expressed as

$$2 \sqrt[N]{\varepsilon} \leq \exp \left(- \left(\frac{1}{\sqrt{32\sigma_x^2}} \ln \left(\frac{\bar{\gamma} e^{4\mu_x}}{2C_\varepsilon - 1} \right) \right)^2 \right) \quad (60)$$

After some further simplification, the lower bound of outage capacity and throughput can be stated

$$C_\varepsilon \geq \log_2 \left(1 + \bar{\gamma} e^{4\mu_x} \exp \left\{ -\sqrt{-32\sigma_x^2 \ln \left(2 \sqrt[N]{\varepsilon} \right)} \right\} \right) \quad (61)$$

$$T_\varepsilon \geq (1 - \varepsilon) \log_2 \left(1 + \bar{\gamma} e^{4\mu_x} \exp \left\{ -\sqrt{-32\sigma_x^2 \ln \left(2 \sqrt[N]{\varepsilon} \right)} \right\} \right) \quad (62)$$

4.4 Numerical Results and Discussions

In this section, we present the outage capacity of derived expressions and show the effects of distance, number of users and average SNR on outage capacity variation through select-max scheduling technique on multiuser FSO system. We assume an FSO system with $\lambda=1550$ nm under clear weather conditions with a visibility of 10 km. The distance between the transmitter and the receivers are assumed to be varied between 2.5 km to 3.5 km. Furthermore, we consider an atmospheric attenuation of 0.42 dB/km (i.e., $\tau \approx 0.1$) and refraction structure parameter of $C_n^2 = 1 \times 10^{-14} \text{m}^{-2/3}$.

In Fig.9, we illustrate the outage capacity versus average SNR of FSO system under the assumption of both iid and inid channel model for a multiuser system with $N=10$ receives. As it can be observed when all users are distributed non-identically, i.e., receivers are located in distance of 2.5 km to 3.5 km from the transmitter, the outage capacity will be got the value between maximum and minimum outage capacity of a system where for the case of maximum and minimum outage capacity, receivers are located equidistantly in 2.5 km and 3.5 km of the transmit node, respectively. Moreover, the lower bound of outage capacity for inid scenario has been illustrated in Fig. 9. As it can be understood from the figure, based on the comparison of outage capacities for both iid systems and inid one. Based on the target outage capacity, i.e., $C_\epsilon = 7$ bits/s/Hz, the required average SNR when the receivers are placed equidistantly in 2.5 km and 3.5 km of transmit node under iid assumption and non-equidistantly placed between 2.5 km to 3.5 km of the transmit node for inid scheme are 11.5 dB, 15 dB and 18 dB, respectively.

Fig. 10 depicts the analytical outage capacity versus average SNR for the case of iid channel model within different placement of receivers. We further presents the obtained lower bound outage capacity of the system under the consideration. As it can be revealed from Fig. 10, path loss has a significant effect on the performance of proposed FSO system. For instance, in the system which receivers are located

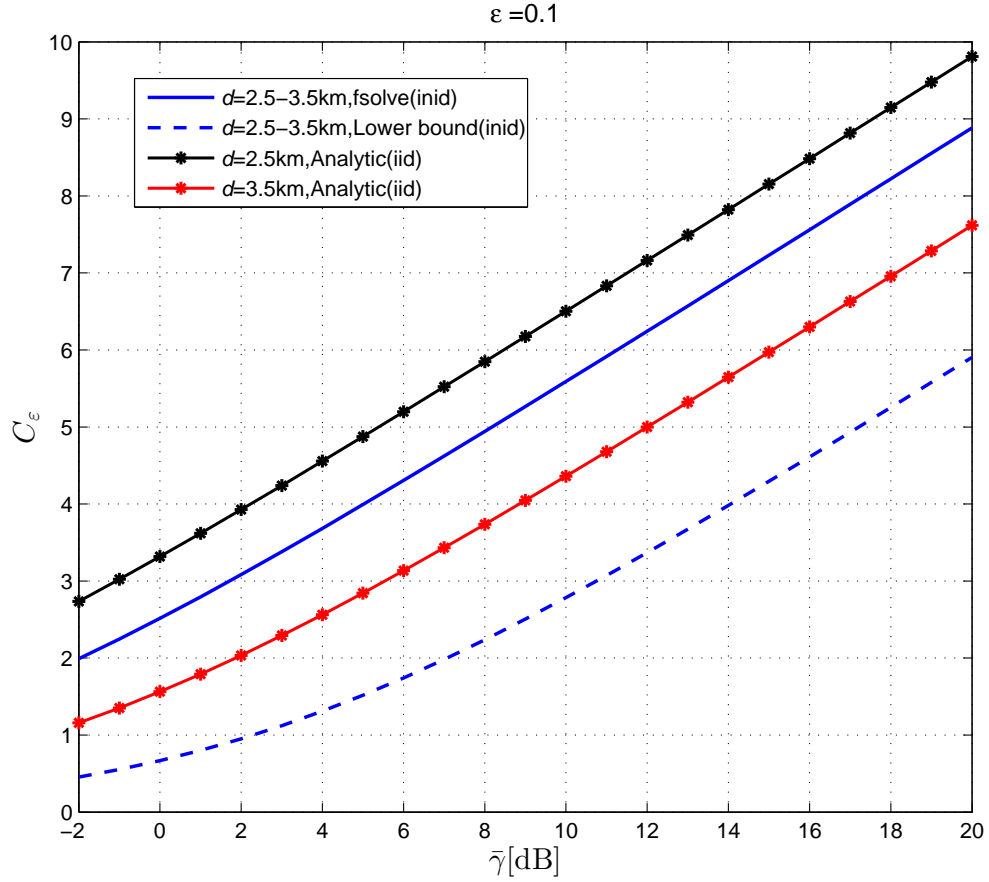


Figure 9: Outage Capacities of Multiuser FSO system, considering max-select scheduling protocol with $N = 10$ have been shown for iid cases of $d = 2.5$ km and $d = 3.5$ km. Furthermore the iid case of placing users over the boundary of 2.5 km to 3.5 km along with the lower bound of corresponding outage capacities are presented.

in a closer distance from the transmitter, i.e., 2.5 km, the outage capacity of $C_\epsilon = 7$ bits/s/Hz can be achieved in 12 dB of average SNR, on the contrary, when the distance of receivers increased to 3.5 km, the required average SNR increased by 6 dB for the same target outage capacity. Also, as it can be seen in Fig. 10, as the average SNR increases, the lower bound outage capacity follows the outage capacity with much more identical trend.

Fig. 11 shows the outage capacity versus number of users for different scenarios of low and high average SNR regime. As it can be seen in the figure, increasing the

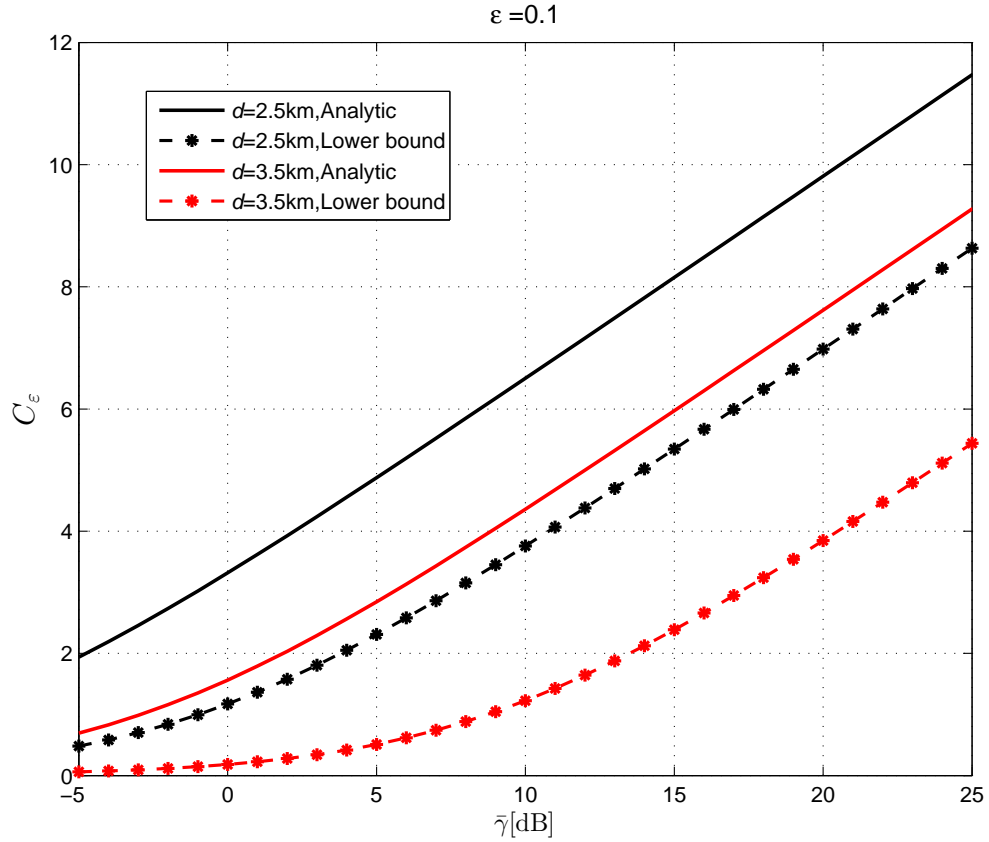


Figure 10: Outage Capacities of Multiuser FSO system, assuming max-select scheduling protocol with $N = 10$ are included for iid cases of $d = 2.5$ km and $d = 3.5$ km along with the lower bound of each outage capacity.

number of users leads to higher performance results in addition to the significant impact of shorter distance from the transmitter on the outage capacity of the considered system. Furthermore, based on the presented outage capacity versus number of users in two average SNR regime, it can be intuitively found out the better performance results are achievable in higher average SNR. In order to provide better understanding of the figure, we employ an example of required number of users for a target outage capacity as follows, the described system with $N = 10$ users can achieve the outage capacity of $C_\epsilon = 0.8$ bits/s/Hz and $C_\epsilon = 2$ bits/s/Hz for average SNR = -5 dB under the consideration of 3.5 km and 2.5 km, respectively. Also, for high average SNR regime, i.e., 15 dB, the outage capacity is respectively increased to $C_\epsilon = 6$ bits/s/Hz

and $C_\epsilon=8.2$ bits/s/Hz for users location of 3.5 km and 2.5 km, respectively.

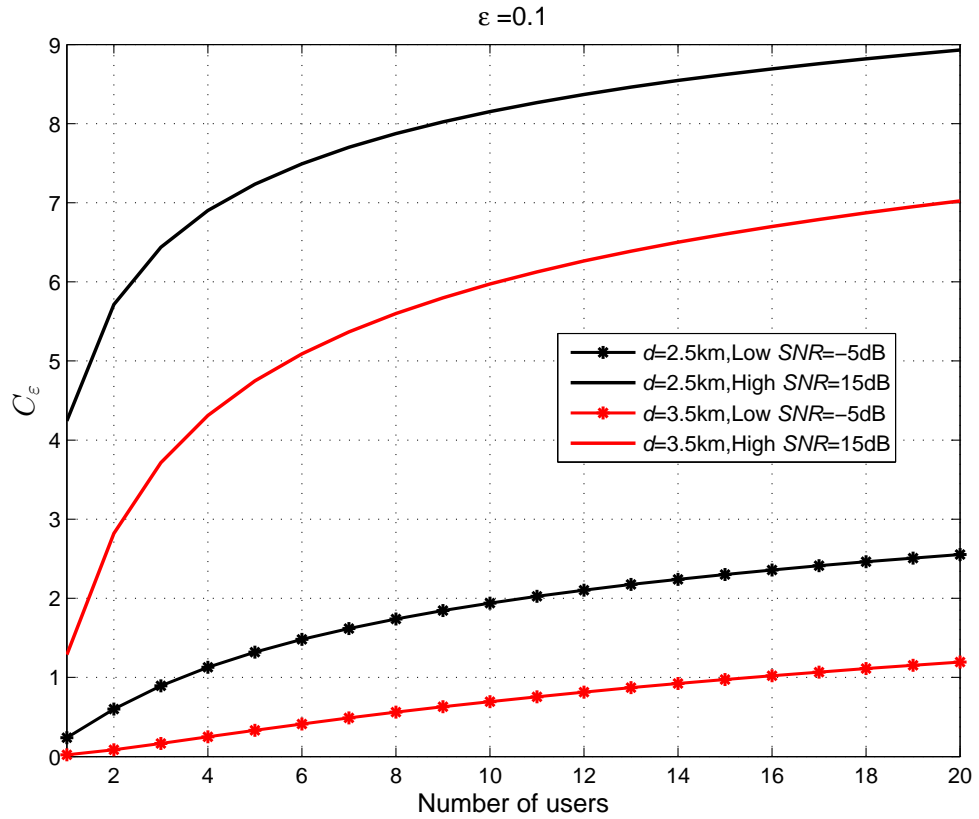


Figure 11: Outage Capacities of multiuser FSO system, assuming max-select scheduling protocol with respect to the number of users are shown for iid cases of $d=2.5$ km and $d=3.5$ km within low and high SNR regimes (-5 dB and 15 dB).

CHAPTER V

CONCLUSION

In this thesis, we have worked on the performance analysis of multiuser FSO communications. We have assumed different schemes of multiuser, including SISO and MIMO and then we extended our work to parallel multihop (cooperative) communications. The performance of the proposed systems has been studied with respect to different metrics involving outage probability, diversity order, outage capacity and throughput. Under the assumption of log-normal channel model, the obtained closed-form expressions have been verified through Monte Carlo simulations.

In the first chapter of this work, we had a review over FSO technology and the advantages come along it. We also took a look over drawbacks of FSO communications and discussed about wide range of mitigation techniques which have been proposed for FSO transmission.

Then, in the next chapter, we studied the outage performance of multiuser FSO communications under log-normal channel model with respect to RR, ORR, select-max and m-BPS protocols and we further investigated the influence of MIMO technique (EGC) on the performance enhancement of the multiuser FSO system.

Furthermore, in chapter three, we extended our scenario to the case of parallel multihop FSO systems and under the consideration of log-normal channel model and m-BPS scheduling technique, we derived outage probability. The outage probability has been studied for both independent identical and non-identical distributions. In addition to the obtained outage probability, we calculated the achievable diversity gain which is equal to $(M - m + 1)(N + 1)^{11/6}$. In the expressed diversity order, M is the total number of paths, N is the number of relay on each path and m indicates

the m^{th} best selected path.

Finally, in the last chapter, we introduced outage capacity and throughput for not necessarily identical multiuser FSO systems. We have obtained the outage capacity and throughput and also lower bound of both terms under the assumption of select-max scheduling protocol and log-normal channel model.

Bibliography

- [1] C. Abou-Rjeily and W. Fawaz, “Space-time codes for mimo ultra-wideband communications and mimo free-space optical communications with ppm,” *IEEE J. Select. Areas Commun.*, vol. 26, no. 6, pp. 938–947, Aug. 2008.
- [2] J. Park, E. Lee, and G. Yoon, “Average bit-error rate of the alamouti scheme in gamma-gamma fading channels,” *IEEE Photon. Technol. Lett.*, vol. 23, no. 4, pp. 269–271, May 2011.
- [3] S. Bloom, “The physics of free space optics,” *AirFiber Inc*, pp. 1–22, 2002.
- [4] I. I. Kim, H. Hakakha, P. Adhikari, E. J. Korevaar, and A. K. Majumdar, “Scintillation reduction using multiple transmitters,” in *SPIE, Free-Space Laser Communication Technologies(Photonics West’97)*, pp. 102–113, International Society for Optics and Photonics, 1997.
- [5] J. A. Anguita and J. E. Cisternas, “Experimental evaluation of transmitter and receiver diversity in a terrestrial fso link,” in *IEEE Global Telecommunications Conference Workshops (GC Wkshps ’10)*, pp. 1005–1009, IEEE, 2010.
- [6] G. Yang, M.-A. Khalighi, S. Bourennane, and Z. Ghassemlooy, “Fading correlation and analytical performance evaluation of the space-diversity free-space optical communications system,” *J. Opt.*, vol. 16, no. 3, pp. 035–403, 2014.
- [7] F. Dios, J. A. Rubio, A. Rodríguez, and A. Comerón, “Scintillation and beam-wander analysis in an optical ground station-satellite uplink,” *Appl. Opt.*, vol. 43, no. 19, pp. 3866–3873, Jul. 2004.
- [8] A. Belmonte and J. Kahn, “Capacity of coherent free-space optical links using atmospheric compensation techniques,” *Optics Express*, vol. 17, no. 4, pp. 2763 – 2773, Feb. 2009.
- [9] N. Das, *Optical Communication*. InTech, 2012.
- [10] Z. Ghassemlooy, W. Popoola, and S. Rajbhandari, *Optical wireless communications: system and channel modelling with Matlab*. CRC Press, USA, 2012.
- [11] G. Parry, “Measurement of atmospheric turbulence induced intensity fluctuations in a laser beam,” *J. Mod. Opt.*, vol. 28, no. 5, pp. 715–728, 1981.
- [12] R. L. Phillips and L. C. Andrews, “Measured statistics of laser-light scattering in atmospheric turbulence,” *JOSA*, vol. 71, no. 12, pp. 1440–1445, Dec. 1981.
- [13] L. C. Andrews, R. L. Phillips, and C. Y. Hopen, *Laser beam scintillation with applications*. 2001.

- [14] L. C. Andrews, R. L. Phillips, C. Y. Hopen, and M. Al-Habash, "Theory of optical scintillation," *J. Opt. Soc. Am. A*, vol. 16, no. 6, pp. 1417–1429, Jun. 1999.
- [15] J. W. Goodman, "Statistical optics," *Wiley-Interscience*, vol. 1, p. 567, 1985.
- [16] Z. Xiaoming and J. M. Kahn, "Performance bounds for coded free-space optical communications through atmospheric turbulence channels," *IEEE Trans. Commun.*, vol. 51, no. 8, pp. 1233–1239, Aug. 2003.
- [17] M. Uysal, S. M. Navidpour, and L. Jing, "Error rate performance of coded free-space optical links over strong turbulence channels," *IEEE Commun. Lett.*, vol. 8, no. 10, pp. 635–637, Oct. 2004.
- [18] M. Uysal, J. Li, and M. Yu, "Error rate performance analysis of coded free-space optical links over gamma-gamma atmospheric turbulence channels," *IEEE Trans. Wireless Commun.*, vol. 5, no. 6, pp. 1229–1233, Jun. 2006.
- [19] X. Zhu and J. Kahn, "Free-space optical communication through atmospheric turbulence channels," *IEEE Trans. Commun.*, vol. 50, no. 8, pp. 1293 – 1300, Aug. 2002.
- [20] M. Safari and S. Hranilovic, "Diversity and multiplexing for near-field atmospheric optical communication," *IEEE Trans. Commun.*, vol. 61, no. 5, pp. 1988–1997, May 2013.
- [21] E. J. Lee and V. W. S. Chan, "Part 1: optical communication over the clear turbulent atmospheric channel using diversity," *IEEE J. Sel. Areas Commun.*, vol. 22, no. 9, pp. 1896–1906, Nov. 2004.
- [22] A. A. Farid and S. Hranilovic, "Diversity gain and outage probability for mimo free-space optical links with misalignment," *IEEE Trans. Commun.*, vol. 60, no. 2, pp. 479–487, Feb. 2012.
- [23] T. A. Tsiftsis, H. G. Sandalidis, G. K. Karagiannidis, and N. C. Sagias, "Multi-hop free-space optical communications over strong turbulence channels," in *Proc. IEEE International Conference on Communications (ICC '06)*, vol. 6, 2006.
- [24] M. Safari, M. M. Rad, and M. Uysal, "Multi-hop relaying over the atmospheric poisson channel: Outage analysis and optimization," *IEEE Trans. Commun.*, vol. 60, no. 3, pp. 817–829, Mar. 2012.
- [25] C. Abou-Rjeily and S. Haddad, "Cooperative fso systems: Performance analysis and optimal power allocation," *J. Lightw. Technol.*, vol. 29, no. 7, pp. 1058–1065, Apr. 2011.
- [26] N. D. Chatzidiamantis, D. S. Michalopoulos, E. E. Kriezis, G. K. Karagiannidis, and R. Schober, "Relay selection protocols for relay-assisted free-space optical systems," *IEEE/OSA J. Opt. Commun. Netw.*, vol. 5, no. 1, pp. 92–103, Jan. 2013.

- [27] M. A. Kashani and M. Uysal, "Outage performance and diversity gain analysis of free-space optical multi-hop parallel relaying," *IEEE/OSA J. Opt. Commun. Netw.*, vol. 5, no. 8, pp. 901–909, Aug. 2013.
- [28] S. M. Navidpour, M. Uysal, and M. Kavehrad, "Ber performance of free-space optical transmission with spatial diversity," *IEEE Trans. Wireless Commun.*, vol. 6, no. 8, pp. 2813–2819, Aug. 2007.
- [29] M. Razavi and J. H. Shapiro, "Wireless optical communications via diversity reception and optical preamplification," *IEEE Trans. Wireless Commun.*, vol. 4, no. 3, pp. 975–983, May 2005.
- [30] D. Divsalar, R. Gagliardi, and J. Yuen, "Ppm performance for reed-solomon decoding over an optical-rf relay link," *IEEE Trans. Commun.*, vol. 32, no. 3, pp. 302–305, Mar. 1984.
- [31] J. A. Anguita, M. A. Neifeld, and B. V. Vasic, "Spatial correlation and irradiance statistics in a multiple-beam terrestrial free-space optical communication link," *Appl. opt.*, vol. 46, no. 26, pp. 6561–6571, 2007.
- [32] P. Polynkin, L. Klein, T. Rhoadarmer, A. Peleg, and J. Moloney, "Optimized multi-emitter beams for free-space optical communications through atmospheric turbulence," in *Conference on Lasers and Electro-Optics*, p. CWM3, Optical Society of America, 2007.
- [33] D. C. O'Brien, S. Quasem, S. Zikic, and G. E. Faulkner, "Multiple input multiple output systems for optical wireless: challenges and possibilities," in *SPIE Optics+ Photonics*, pp. 630416–630416, International Society for Optics and Photonics, 2006.
- [34] S. G. Wilson, M. Brandt-Pearce, Q. Cao, and M. Baedke, "Optical repetition mimo transmission with multipulse ppm," *IEEE J. Select. Areas Commun.*, vol. 23, no. 9, pp. 1901–1910, Sept. 2005.
- [35] M. Al-Habash, R. Phillips, and L. Andrews, "Mathematical model for the irradiance probability density function of a laser beam propagating through turbulent media," *Optical Engineering*, vol. 40, no. 8, pp. 1554–1562, 2001.
- [36] N. Cvijetic, S. G. Wilson, and M. Brandt-Pearce, "Performance bounds for free-space optical mimo systems with apd receivers in atmospheric turbulence," *IEEE J. Select. Areas Commun.*, vol. 26, no. 3, pp. 3–12, 2008.
- [37] M. A. Khalighi and M. Uysal, "Survey on free space optical communication: A communication theory perspective," *Commun. Surveys Tuts.*, vol. PP, no. 99, pp. 1–1, 2014.

- [38] A. Garcia-Zambrana, C. Castillo-Vazquez, B. Castillo-Vazquez, and A. Hiniesta-Gomez, "Selection transmit diversity for fso links over strong atmospheric turbulence channels," *IEEE Photon. Technol. Lett.*, vol. 21, no. 14, pp. 1017–1019, Jul. 2009.
- [39] B. Castillo-Vazquez, A. Garcia-Zambrana, and C. Castillo-Vazquez, "Closed-form ber expression for fso links with transmit laser selection over exponential atmospheric turbulence channels," *IEEE Electron Lett.*, vol. 45, no. 23, pp. 1185–1187, 2009.
- [40] C. Abou-Rjeily, "On the optimality of the selection transmit diversity for mimo-fso links with feedback," *IEEE Commun. Lett.*, vol. 15, no. 6, pp. 641–643, Jun. 2011.
- [41] A. Garc a-Zambrana, C. Castillo-Vazquez, and B. Castillo-Vazquez, "Space-time trellis coding with transmit laser selection for fso links over strong atmospheric turbulence channels," *Optics express*, vol. 18, no. 6, pp. 5356–5366, Mar. 2010.
- [42] M. Khalighi, N. Schwartz, N. Aitamer, and S. Bourennane, "Fading reduction by aperture averaging and spatial diversity in optical wireless systems," *IEEE/OSA J. Opt. Commun. Netw.*, vol. 1, no. 6, pp. 580–593, Nov. 2009.
- [43] A. J. Paulraj, D. A. Gore, R. U. Nabar, and H. Bolcskei, "An overview of mimo communications—a key to gigabit wireless," *Proceedings of the IEEE*, vol. 92, no. 2, pp. 198–218, 2004.
- [44] S. G. Wilson, M. Brandt-Pearce, Q. Cao, and J. H. Leveque III, "Free-space optical mimo transmission with q-ary ppm," *IEEE Trans. on Commun.*, vol. 53, no. 8, pp. 1402–1412, Aug. 2005.
- [45] N. D. Chatzidiamantis, M. Uysal, T. A. Tsiftsis, and G. K. Karagiannidis, "Iterative near maximum-likelihood sequence detection for mimo optical wireless systems," *J. Lightw. Technol.*, vol. 28, no. 7, pp. 1064–1070, 2010.
- [46] A. S. Acampora and S. V. Krishnamurthy, "A broadband wireless access network based on mesh-connected free-space optical links," *IEEE Pers. Commun.*, vol. 6, no. 5, pp. 62–65, Oct. 1999.
- [47] M. Safari and M. Uysal, "Relay-assisted free-space optical communication," *IEEE Trans. on Wireless Commun.*, vol. 7, no. 12, pp. 5441–5449, Dec. 2008.
- [48] S. Arnon, J. Barry, G. Karagiannidis, R. Schober, and M. Uysal, *Advanced optical wireless communication systems*. 2012.
- [49] S. S. Ikki and M. H. Ahmed, "On the performance of cooperative-diversity networks with the nth best-relay selection scheme," *IEEE Trans. on Commun.*, vol. 58, no. 11, pp. 3062–3069, Nov. 2010.

- [50] Y. Liang, G. Xiqi, and M. S. Alouini, “Performance analysis of free-space optical communication systems with multiuser diversity over atmospheric turbulence channels,” *IEEE Photon. J.*, vol. 6, no. 2, pp. 1–17, Apr. 2014.
- [51] A. Goldsmith, *Wireless Communications*. Cambridge University Press, 2005.
- [52] R. Knopp and P. A. Humblet, “Information capacity and power control in single-cell multiuser communications,” in *Proc. IEEE International Conference on Communications (ICC '95)*, 1995.
- [53] D. N. Tse, “Optimal power allocation over parallel gaussian broadcast channels,” in *Proc. IEEE International Symposium on Information Theory*, 1997.
- [54] J. Abouei and K. N. Plataniotis, “Multiuser diversity scheduling in free-space optical communications,” *J. Lightw. Technol.*, vol. 30, no. 9, pp. 1351–1358, May 2012.
- [55] H. Yang and M. Alouini, *Order Statistics in Wireless Communications: Diversity, Adaptation, and Scheduling in MIMO and OFDM Systems*. 2011.
- [56] S. Haas, *Capacity of and Coding for Multiple-Aperture Wireless Optical Communications*. Thesis, 2003.
- [57] L. C. Andrews, R. L. Phillips, and C. Y. Hopen, *Laser beam scintillation with applications*. 2001.
- [58] M. Safari and M. Uysal, “Diversity gain analysis of free-space optical communication systems,” in *Proc. Electrical and Computer Engineering Canadian Conference (CCECE)*, pp. 1239–1244, 2008.
- [59] A. F. Molisch, *Wireless communications*, vol. 15. John Wiley & Sons, 2010.
- [60] S. S. Kulkarni and C. Rosenberg, “Opportunistic scheduling policies for wireless systems with short term fairness constraints,” in *Proc. IEEE Global Telecommunications Conference (GLOBECOM '03)*, vol. 1, pp. 533–537 Vol.1, 2003.
- [61] M. Johansson, “Diversity-enhanced equal access-considerable throughput gains with 1-bit feedback,” in *Proc. IEEE 5th Workshop on Signal Processing Advances in Wireless Communications*, pp. 6–10, 2004.
- [62] V. Hassel, M. R. Hanssen, and G. E. Oien, “Spectral efficiency and fairness for opportunistic round robin scheduling,” in *Proc. IEEE International Conference on Communications (ICC '06)*, vol. 2, pp. 784–789, 2006.
- [63] M. K. Simon and M.-S. Alouini, *Digital communication over fading channels*, vol. 95. John Wiley & Sons, 2005.
- [64] B. C. Arnold, N. Balakrishnan, and H. H. N. Nagaraja, *A first course in order statistics*, vol. 54 of *Classics in Applied Mathematics*. Philadelphia, USA: SIAM, 2008.

- [65] N. Balakrishnan, “Permanents, order statistics, outliers, and robustness,” *Revista matemática Complutense*, vol. 20, no. 1, pp. 7–107, 2007.
- [66] M. Safari and M. Uysal, “Cooperative diversity over log-normal fading channels: performance analysis and optimization,” *IEEE Trans. on Wireless Commun.*, vol. 7, no. 5, pp. 1963–1972, May 2008.
- [67] M. Chiani, D. Dardari, and M. K. Simon, “New exponential bounds and approximations for the computation of error probability in fading channels,” *IEEE Trans. on Wireless Commun.*, vol. 2, no. 4, pp. 840–845, Jul. 2003.
- [68] M. A. Kashani, M. Safari, and M. Uysal, “Optimal relay placement and diversity analysis of relay-assisted free-space optical communication systems,” *IEEE/OSA J. Opt. Commun. Netw.*, vol. 5, no. 1, pp. 37–47, Jan. 2013.
- [69] A. S. Avestimehr and D. N. C. Tse, “Outage capacity of the fading relay channel in the low-snr regime,” *IEEE Trans. Inform. Theory*, vol. 53, no. 4, pp. 1401–1415, Apr. 2007.
- [70] Z. Xing, L. Zhaobiao, and W. Wenbo, “Performance analysis of multiuser diversity in mimo systems with antenna selection,” *IEEE Trans. on Wireless Commun.*, vol. 7, no. 1, pp. 15–21, Jan. 2008.
- [71] S. M. Haas and J. H. Shapiro, “Capacity of wireless optical communications,” *IEEE J. Select. Areas Commun.*, vol. 21, no. 8, pp. 1346–1357, Oct. 2003.
- [72] A. A. Farid and S. Hranilovic, “Outage capacity for miso intensity-modulated free-space optical links with misalignment,” *IEEE/OSA J. Opt. Commun. Netw.*, vol. 3, no. 10, pp. 780–789, Oct. 2011.
- [73] A. A. Farid and S. Hranilovic, “Outage capacity optimization for free-space optical links with pointing errors,” *J. Lightw. Technol.*, vol. 25, no. 7, pp. 1702–1710, Jul. 2007.
- [74] D. Tse and P. Viswanath, *Fundamentals of wireless communication*. Cambridge University Press, UK, 2005.
- [75] R. Wonjong and J. M. Cioffi, “On the capacity of multiuser wireless channels with multiple antennas,” *IEEE Trans. Inform. Theory*, vol. 49, no. 10, pp. 2580–2595, Oct. 2003.
- [76] J. Proakis and M. Salehi, *Digital Communications*. McGraw–Hill, New York, USA, 2008.
- [77] S. Furrer, P. Coronel, and D. Dahlhaus, “Simple ergodic and outage capacity expressions for correlated diversity rician fading channels,” *IEEE Trans. on Wireless Commun.*, vol. 5, no. 7, pp. 1606–1609, 2006.

- [78] C. Chen, B. Lin, W. Bo, and C. Jinho, "Downlink throughput maximization for ofdma systems with feedback channel capacity constraints," *IEEE Trans. Signal Processing*, vol. 59, no. 1, pp. 441–446, Jan. 2011.

VITA

Sasan Zhalehpour received B.Sc. and M.Sc. degrees in Electrical Engineering from Iran University of Science and Technology (IUST), Tehran, Iran in 2005 and 2009, respectively. He is currently working toward the M.Sc. degree in Electrical and Electronics Engineering Department at Ozyegin University, Istanbul, Turkey. He is member of CT&T Research Group headed by Professor Murat Uysal. His research interests include Physical Layer Aspects of Wireless Communication Systems, Wireless (Free Space) Optical Communications, Cooperative Transmission, MAC Protocols.